COMBINATORIAL CODING OF SALT TASTE IN THE FLY LABELLUM

by

Alexandria Jaeger

B.Sc., The University of Nevada, Reno, 2014

A THESIS SUBMITTED IN PARTIAL FULFILLMENT OF

THE REQUIREMENTS FOR THE DEGREE OF

MASTER OF SCIENCE

in

THE FACULTY OF GRADUATE AND POSTDOCTORAL STUDIES

(Neuroscience)

THE UNIVERSITY OF BRITISH COLUMBIA

(Vancouver)

April 2017

Abstract

Salt is an important component of most of the food we ingest daily, yet its detection in food and the control of its consumption remain poorly understood. The gustatory system of an animal underlies the processing of salt taste. With the ability to taste on multiple parts of the body, *Drosophila melanogaster* makes critical decisions about beneficial tastants to consume, and potentially harmful tastants to avoid. Most chemicals sensed by the gustatory system drive either attraction or repulsion, but salt is unique in that it is appetitive at low concentrations and repulsive at high concentrations. How salt is encoded, processed, modulated, and drives behavior is still not well defined. Through immunolabeling, calcium imaging, and a variety of behavioral assays, we are working on understanding these questions. I have constructed a taste sensory neuron map by co-labeling different gustatory receptors and protein markers for the neurotransmitters glutamate and acetylcholine.

Interestingly, while most sensory neurons are cholinergic, I have found that the ENaC family member ppk23 labels a population of glutamateric taste neurons in the fly labellum (the analog of the mammalian tongue). Using calcium imaging, I have characterized the responses of this and other major populations of taste sensory neurons, and found that most, if not all, taste sensory neurons respond to salt in some way. We look at the effect of salt deprivation on sugar and salt sensing labellar GRNs' physiology to further understand the neural circuitry devoted to this salt sensing pathway. This work challenges the current paradigm of labelled lines coding in the gustatory system of flies, and instead presents evidence of combinatorial coding in salt. Understanding the basic neural circuitry in the fly gustatory system and how that drives behavior in the face of different internal states across modalities, will give insight into how taste information is translated into appropriate feeding responses.

Preface

This work was executed at UBC's Life Science Institute by Alexandria Jaeger and Dr. Michael Gordon. Dr. Gordon designed and supervised the project. All questions and project directions were constructed in collaboration between Dr. Gordon and I. I performed all the immunohistochemically and calcium imaging experiments. I conducted all analysis for all of the experiments, as well as quantified data using ImageJ and Microsoft Excel, and ran statistical analysis in GraphPad Prism 6. Introductory figures in Chapter 1 (Figures 1.1 and 1.2) were produced and adapted from Dr. Gordon. Labellum schematic in chapter 1 and 3 (Figures 1.4, 3.1, 3.2, 3.4) were adaptations from Wiess LA et al. (2011). Neuron schematic in chapter 3 (Figure 3.5 and Figure 3.9) were adaptations from Freeman EG and Dahanukar A (2015). I graphed all curve average's in the figures in Chapter 3 (Figures 3.5 and 3.6) with GraphPad Prism 6 and the layout was constructed in Adobe Illustrator by Pierre-Yves Musso. Figure 3.8A shows the experimental set up for salt deprivation which was reproduced and adapted from Pierre-Yves Musso. Figure 3.9C circuit diagram was produced and adapted from Dr. Gordon. I created all other figures with experiments I conducted.

List of Figures

List of Abbreviations

7-T	7-tricosene
7,11-HD	7,11-heptacosadine
7,11-ND	7,11-nonacosadiene
AHL	adult hemolymph-like
AL	antennal lobe
AMMC	antennal mechanosensory and motor center
AP	action potential
C	Celsius
Ca^{+}	calcium
CaM	calcium binding protein calmodulin
CHC	cuticular hydrocarbons
CNS	central nervous system
CO_2	carbon dioxide
cpGFP	circularly permuted GFP
cVA	11-cis vaccenyl acetate
DCSO	dorsal cibrarial sense organ
ddH2O	double distilled water
DNA	deoxyribonucleic acid
ENaC	Epithelial sodium channel
EtOH	ethanol
F	fluorescence
fru^{+}	fruitless positive

GABA	λ-Aminobutyric acid
GECI	genetically-encoded calcium indicator
GFP	green fluorescent protein
GPCR	G-protein coupled receptor
GRASP	GFP reconstitution across synaptic partners
Gr	Gustatory receptor
GRN	Gustatory receptor neuron
I	intermediate
IR	ionotropic glutamate receptor
KCl	potassium chloride
KIR2.1	inwardly rectifying potassium channel 2.1
L	long
LSO	labral sense organ
M	molar
Mg^{2+}	magnesium
mM	milimolar
MN	motorneuron
mRNA	messenger RNA
ms	milliseconds
MSG	monosodium glutamate
Na^{+}	sodium
NaCl	sodium chloride
ns	not significant

NT	neurotransmitter
OR	olfactory receptor
ORN	olfactory receptor neuron
PER	proboscis extension reflex
PFA	paraformaldehyde
PI	preference index
ppk	pickpocket
$ppk23^{+}/gr66a^{+}$	Neurons positive for both *ppk23-gal4* and *gr66a-gal4*
RNAi	ribonucleic acid (RNA) interference
s	seconds
S	short
SEM	standard error of the mean
SEZ	subesophageal zone
sGPNs	sweet gustatory projection neurons
siRNA	short interfering RNA
sNPF	short neuropeptide F
SP	Sex Peptide
SPSN	Sex Peptide Sensory Neurons
TO	terminal organ
TRC	taste receptor cells
UAS	upstream activating sequence
uM	micromolar
VCSO	ventral cibraial sense organ

Acknowledgements

I would like to express the endless amount of appreciation I have for my supervisor and mentor Mike Gordon. Thank you for believing in me, for pushing me, and for engaging me in conversation and thought. Thank you for answering all my questions, no matter how ignorant, with minimal eyebrows raised. I would also like to thank my supervisory committee, Dr. Vanessa Auld, Dr. Elizabeth Rideout, and Dr. Catharine Rankin, for all the suggestions and feedback on this thesis project. I appreciated all the time you gave me, it was a pleasure interacting with such bright and motivated women.

I would like also like to thank all the members of Gordon lab that I interacted with over the years. Thank you for all the help both in and out of the lab. I have become a better scientist because of every one of you. Thank you to Bonnie Chu and Dr. Emily LeDue for showing me the ropes and teaching me how to be a productive, efficient, and positive (at times negative) contributing member of the scientific community. Thank you for all the laughs, for teaching me how to navigate free food, caffeine, and alcohol on campus, and of course for all the cat parties. Thank you to Dr. PYM(adonna) who could not have showed up at a more necessary time, who has taught me how to be confident and focused in my science. Thank you for re-instilling curiosity and excitement in me. Thanks to Marie for all the wisdom and interesting conversations. Thank you to the beautiful and kind Dr. Mary Pines. You welcomed me when I had no one and have helped me become the person I am today. Thank you for all the dancing and conversations, for pushing the importance of a work-life balance.

Thank you to my neuroscience community, you guys are my family and helped keep me sane throughout this whole process. Thanks for all the long days, late nights, camping trips, road trips, and random moments that truly helped to make Vancouver my home. Thanks to my best friends Lily, Bryce, Harrison, Cam, Maya, Stefano, Sarah, Troy, Christine, and Lily (number two, but no less special), I cannot put into words what you guys mean to me. You all have supported my craziness only to make me feel completely normal.

Thank you to my best friends near and far who have continued to give me support over all the years: Elliot, Catherine, Sarah, Junshi, Michael, Edmund, Paola, and Josie. It does not matter how often we talk, or how far away we are, your support has never gone unnoticed.

Thank you to my family. Thanks to my grandparents who think that everything I do is deserving of a special award. Thanks to my mom who has always pushed to live a life full of meaning. Thanks to my favorite Aunt, your free spirit has always driven me to approach life with an open mind. Thanks to grandpa Morrie, you're my biggest cheerleader and I could not love you more; thank you for making my life as easy as possible.

Thanks to my dad who has always been my rock, whom without I would have never gotten here. Thanks for instilling my love of libraries and learning. Thank you for always believing that I will make the right decision, even when I obviously do not. Thank you for navigating through my breakdowns even from far away. Thank you for pushing me, for encouraging me, and for celebrating my independence.

1 Introduction

1.1 The fly gustatory system

The gustatory neural network of an animal is fundamental to life. The common fruit fly, *Drosophila malanagaster* is no exception to this rule, as its ability to taste its surrounding environment and make decisions about what to consume will ultimately determine its fitness. With the fly brain being composed of only about 200,000 neurons, it is important that the circuitry segregated to the gustatory system be efficient from the initial contact with sensory neurons through to the rejection or acceptance of feeding. A small number of neurons, paired with a large number of behaviors, in addition to the available genetic manipulations, makes the fruit fly an ideal model to answer important questions about the gustatory neural networks of animals. An understanding of how neural circuitry is constructed and regulated in a model organism is a foundation on which to understand mammalian neural networks.

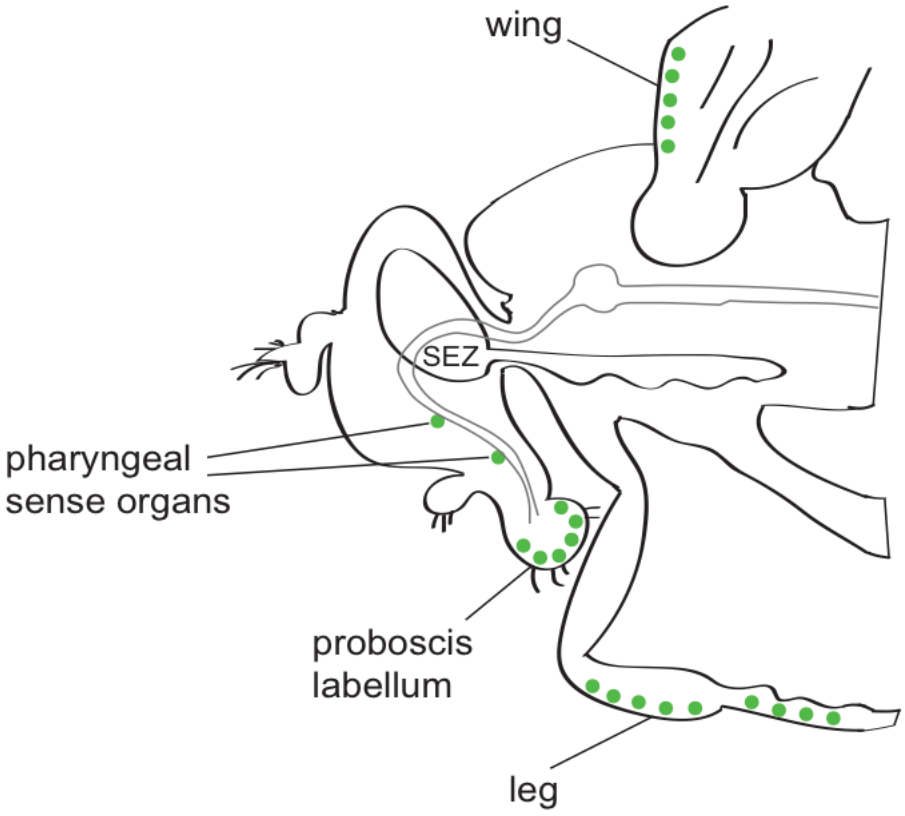

Figure 1. 1 Gustatory organs in the adult fly
The adult fly senses tastants in the environment through sensilla located on the legs, wings, ovipositor (not shown), and proboscis. More specifically for the proboscis, sensilla are found at the exterior tip called the labellum, and on the pharynx, separated into the dorsal and ventral cibarial sense organs. All neurons in sensilla send axon projections to the taste area of the brain known as the subesophageal zone (SEZ) (adapted by Michael D. Gordon from Chu, 2014).

1.1.1 Anatomy of gustatory organs

The fly has the ability to taste on many different parts of its body; the wings, the legs, the proboscis, and the ovipositor all house neurons responsible for sending taste information to the brain (Figure 1.1., Stocker, 1994; Gendre et al., 2004). The legs and the proboscis house many neurons and can be considered the primary fly taste organs (Scott et al., 2001). The proboscis, a tubular extendable appendage on the fly head, is the feeding structure where the fly ultimately makes its decision of whether or not to ingest food (Stocker, 1994). At the end of the proboscis is

the labellum, analogous to the mammalian tongue, which is made up of two labellar palps decorated with taste hairs and lined with rows of taste pegs between pseudotracheae (Stocker, 1994). Inside the proboscis lies the pharynx, which also has gustatory neurons that respond to tastants once the fly has ingested a substance (LeDue, 2015). The pharynx is separated into three different, bilaterally symmetric, pharyngeal sense organs (Gendre et al., 2004). Along the upper and middle segment of the pharynx lie the dorsal and ventral cibarial sense organ (DCSO and VCSO) respectively, and distally along the hypopharynx lies the labral sense organ (LSO) (Gendre et al., 2004). The female fly also has specific gustatory receptors on the ovipositor, which it may use to probe a medium in deciding where best to lay her egg (Yang et al., 2008). This is important as the survival of her offspring is dependent on the nutrients in the food where the larvae hatches from the egg.

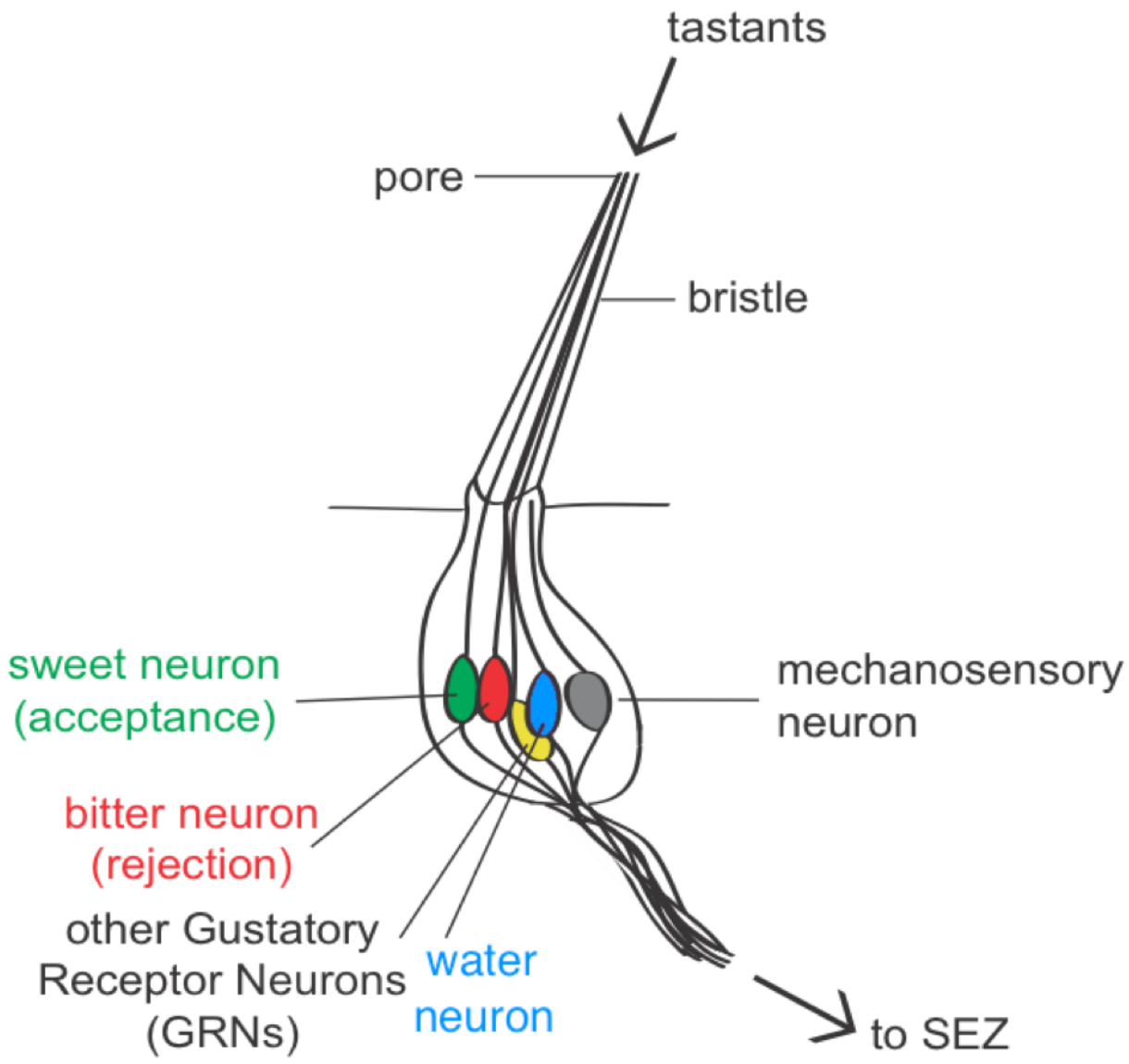

Figure 1. 2 Gustatory receptor neurons in a taste sensillum
Each taste sensillum (taste hair) is comprised of 2-4 gustatory receptor neurons characterized by the expression of gustatory receptors expressed by each neuron. Generally, each hair has one sweet neuron (Gr64f), one bitter neuron (Gr66a), one water neuron (ppk28), and one additional GRN. Each taste hair also has one mechanosensory neuron. All neurons extend their dendrites out into the periphery to make contact with different tastants in the environment, and send their axons into the taste area of the brain, the subesophageal zone (adapted from Chu, 2014).

In each taste organ of the fly, exists a series of sensilla, or taste hairs. These taste hairs house the neurons that are the first responders to different tastants in the environment, similar to taste buds on a mammalian tongue (Stocker, 1994). Each sensillum is comprised of a range of 2-

4 neurons, which are characterized by the composition of gustatory receptors expressed by each neuron (Figure 1.2). In addition to the gustatory receptor neurons (GRNs), each sensillum also contains a mechanosensory neuron (MN) responsible for sensing texture, which plays an important role in feeding decisions (Jeong, 2016). There are additional accessory cells, which are not directly involved in taste detection (Andrés et al., 2014; Kawano et al., 2015). The distribution of sensilla over the fly's body influences each organ's sensitivity to discrete tastants. For instance, the distal segment (tarsi) of the first legs have a higher concentration of sensilla, and thus receptors, than the proximal area of the same legs, allowing them to better distinguish differences in stimuli (Stocker, 1994; Freeman and Dahanukar, 2015).

Taste hairs on the labellum are grouped into three families based on their size and neuron composition: Short (S-type), intermediate (I-type), and long (L-type) sensilla (Stocker, 1994). All three contain one appetitive neuron that responds to sweet stimuli and drives acceptance behavior, as well as one aversive neuron that usually responds to bitter stimuli and drives repulsive behavior (Stocker, 1994). The cell body of these neurons sit in the bristle shaft and the dendrites extend out into the periphery to make contact with different tastants. The axons extend into the subesophageal zone (SEZ) of the brain, where they are segregated to create a gustatory map (Stocker, 1994). These projections are segregated not only by where on the body the fly is tasting, but also what tastant the fly is tasting (Wang et al., 2004). The fly has the ability to distinguish between an array of different molecules and concentrations, but most gustatory receptor neurons are dedicated to sensing sweet, bitter, or salt (Hiroi, et al., 2002; Hiroi, et al., 2004; Freeman and Dahanukar, 2015).

When any of these taste organs come in contact with something appetitive that the fly would like to ingest, it can extend its proboscis and consume the compound. This behavior is

recognized as the proboscis extension reflex (PER), which consists of a reliable contraction of muscles that propel the feeding structure in the direction of a food source (Rajashekhar and Singh, 1994b). This reflex can be reversed by one of the taste organs making contact with a repulsive substance, causing a retraction of the proboscis. Due to the consistency of this feeding behavior and its easily observable phenotype, it is a favorite measurement of taste acceptance.

1.1.2 Gustatory receptors

Each GRN population has a specific array of receptors that tune the neurons to specific chemical species. Each GRN generally expresses a collection of receptors that bind a similar class of ligands, and thus, each neuron population is defined by the ligands that activate these receptors (Scott et al., 2001). The largest number of proteins from the gustatory receptor (GR) family of genes are found in the labellum. Between the larvae and adult 68 GR candidates were found, each a seven-transmembrane protein (Scott et al., 2001; Robertson et al., 2003).

By examining GR expression, we can begin to understand the coding of tastes in peripheral organs. Importantly, opposing taste modalities generally do no activate the same neuron populations, as bitter and sweet molecules bind to distinct groups of GRs (Wang et al., 2004). This can be observed when looking at the expression pattern of Gr64f, which is expressed in all sugar sensing neurons (Jaio et al., 2008). This sugar receptor does not have any overlap in the expression pattern of Gr66a, a receptor expressed in all bitter sensing neurons (Wang et al., 2004; Thorne et al., 2004; Weiss et al., 2011). Many of the sugar GRs are necessary and sufficient for tasting a wide array of sugar molecules; however, some receptors are more narrowly tuned, and some sugars are less promiscuous, eliciting responses to fewer receptors (Dahanukar et al., 2001). Additionally, Gr64f has found to be necessary to evoke a sugar response with all sugars except fructose (Dahanukar et al., 2007; Jaio et al., 2008). One GR has

been identified, Gr43a, that responds to dietary fructose in the brain and acts as a nutrient sensor (Miyamoto et al., 2012). Interestingly, when these receptors are expresses ectopically in naïve cells they are unresponsive to their characterized ligand, indicating that these GRs function in a complex (Jaio et al., 2008).

Although sweet and bitter are the most well studied taste modalities, additional receptors responsible for other modalities have also been identified. A water sensing neuron is also found in most sensilla (Stocker, 1994). This neuron houses a different kind of taste receptor, a Degenerin (Deg)/Epithelial sodium channel (ENaC) from the pickpocket gene family, ppk28, which is a sensor for low osmolality (Cameron et al., 2010; Jourjine et al., 2016). Interestingly, this family of ion channels is responsible for detection of low sodium taste in mammals (Chandrashekar et al., 2010). The final most abundant cell in the sensillum is thought to be dedicated to salt sensation. However, there is evidence that salt evokes responses from more GRN types than just this dedicated population. It is known that flies, like mammals, are attracted to low concentrations of salt but as the concentration increases, salt becomes aversive. Because low salt is appetitive, most of this attraction is attributed to the sugar sensing cell (Hiroi et al., 2002). Similarly, because high salt is repulsive, most aversion has been attributed to high salt activating the bitter sensing cell; although, it is widely understood that an additional repellant neuron population is still uncharacterized (Hiroi et al., 2002; Freeman and Dahanukar, 2015). Additionally, an ionotropic glutamate receptor Ir76b was found to also be necessary for low salt attraction, now thought to be mediated specifically by the L-type sensilla (Zhang et al., 2013; Ganguly et al., 2017). However, this receptor is in a range of both olfactory and gustatory neurons so the exact neuronal population in which it functions is debated (Hussain et al., 2016, Freeman and Dahanukar, 2015).

Many other receptors in the gustatory system have been found to bind an assortment of different tastants that are important for the fly to recognize. A series of ENaCs, ppk25, ppk29, ppk23, have been shown to label pheromone-sensitive GRNs, and are necessary for the pheromone responses (Kallman et al., 2015; Toda et al., 2012; Thistle et al., 2012). Ir76b is responsible for tasting amino acids in the larvae, as well as sensing polyamines through both taste and olfaction (Croset et al., 2016; Hussain et al., 2016). Ir76b has also been shown to be necessary for amino acid taste in the legs of adults, working in a complex with Ir20a to make the population functionally exclusive (Ganguly et al., 2017). Acidic substances have been found to be repulsive, so detecting difference in pH is important for the fly. Neuron populations show responses to low pH, but when receptors in these deterrent neurons are knocked down no effect is seen on acid detection (Freeman and Dahanukar, 2015). The enzyme phospholipase C in sweet sensing neurons is necessary for fatty acid detection, but the receptor in which it acts on is still unknown (Mastic and Keene 2013). Ammonia, a popular attractant among insects, can be sensed by an Amt^+ GRN population (Delventhal et al., 2017).

Not all members of the GR family have been found to be expressed in GRNs or respond to tastants. Gr21a and Gr63a, expressed in fly olfactory receptor neurons (ORNs), have been shown to sense CO_2 in the environment (Kwon et al., 2007; Fischler et al., 2007). Interestingly, although CO_2 is aversive to flies, the homologs of these receptors mediate the attraction of mosquitoes to CO_2 (Jones et al., 2007). The receptor Gr28b(D), found in the arista (feather like appendage on the antennae), is a thermosensor, responding to heat (Ni et al., 2013). Another stimulus that GRs have been shown to respond to is specific photon wavelengths. In larvae, Gr28b is expressed in the body and is required to deter the animal from noxious light (Xiang et al., 2011). All these GR genes were originally identified by a signature motif in the carboxyl

terminus of the seventh transmembrane domain of potential proteins, by polymerase chain reaction (PCR) analysis of labellar ribonucleic acid (RNA) (Scott et al., 2001). These extracurricular GRs are important for the fly to engage in its environment in a healthy way. With new GRs emerging that do not respond to classic tastants, it is clear that the GR family, and possibly gustatory coding, are more complex than originally thought.

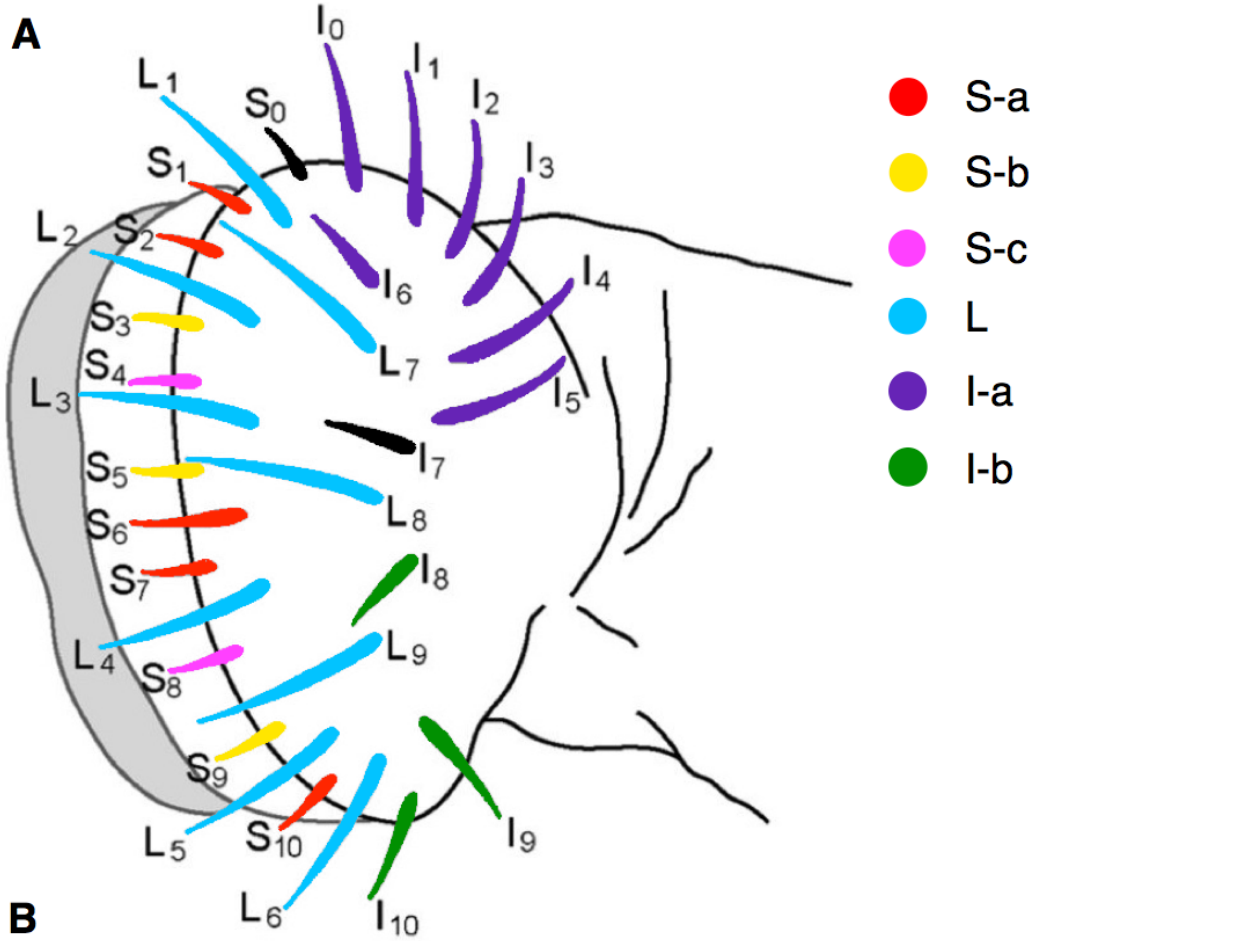

Figure 1. 3 Sensillum types on the adult fly labellum
Taste hair and neuron number distribution across the labellum. (A) 31 sensilla on a single labellar palp can be broken down into five different groups depending on which neuron populations are present. (B) Number of GRNs present in the different groups of taste hairs (adapted from Weiss LA., 2014; Freeman EG and Dahanukar A., 2015).

1.1.3 Sensilla in the fly labellum

By taking a closer look at the primary taste organ, the labellum of the fly, a better understanding of taste distribution at a sensory level can be understood. Each of the two symmetrical labellar palps houses 31 sensilla (Figure 1.3; Stocker, 1994). The S-type sensilla line the lower edge of the labella, which lies more medially on the proboscis. There are eleven S-type sensilla, numbered from S0-S10. The L-type are in the middle of the palp and are numbered L1-L9. Each of the S- and L-type sensilla have four GRNs plus one MN. As previously described, one neuron dedicated to sweet sensing and one to bitter sensing, in addition to one osmolality sensing, with the last neuron differing between different taste hairs (Stocker, 1994; Freeman and Dahanukar, 2015). The I-type are on the upper edge of labella and lay more laterally, numbered I0-I10. These hairs differ from the other types as they only have two GRNs: one sweet and one bitter neuron (Stocker, 1994; Freeman and Dahanukar, 2015). Originally it was thought that all sensilla type could be considered equal, but with the dissection of each receptor's expression and the response pattern of each taste hair, a more complicated story emerges (Hiroi et al., 2002; Hiroi et al., 2004; Weiss et al., 2011).

The S-type sensilla can be further broken down into three groups based on receptor expression: S-a, S-b, and S-c (Freeman and Dahanukar, 2015). S-a (S1, S2, S6, S7, S10) contains a sweet sensing neuron with many sweet GRs, a bitter sensing neuron with many bitter GRs, and a water sensing neuron with ppk28. The fourth neuron in these sensilla has been proposed to be a ppk23-expressing pheromone GRN, but this has not been confirmed (Freeman and Dahanukar, 2015; Thistle et al., 2012). S-b (S3, S5, S9) sensilla are very similar to S-a sensilla, with the

exception that they have fewer bitter receptors in the bitter cell (Weiss et al., 2011). S-c (S4 and S8) sensilla have the same receptors expressed in the sugar cell, water cell, and proposed pheromone cell, making these neuron populations ubiquitous among the S-type hairs. However, S-c sensilla do not have a bitter sensing neuron and instead have an uncharacterized neuron population (Freeman and Dahanukar, 2015). This description leaves out S0 as it is inconsistently present and very hard to record from.

All nine L sensilla have the same GR expression in each respective cell. As with the S-type, one cell expresses ppk28 and senses osmolality. The sugar sensing neuron has an array of sugar GRs, some overlapping with previous populations mentioned in S-type, but still unique as some addition receptors are present. One cell is considered to be the low salt cell, expressing only Ir76b (Ganguly et al., 2017; Zhang et al., 2013). The last cell is an uncharacterized cell, thought to be unique from the unknown cell in S-c type sensilla (Freeman and Dahanukar, 2015).

The I-type sensilla are further separated into two populations: I-a and I-b (Freeman and Dahanukar, 2015). I-a (I0-I6) exist more superior on the labellum, with a sugar neuron that expresses the smallest, yet still abundant, collection of receptors. There are ubiquitous receptors between all sugar populations, but this neuron group is still unique from previously discussed GRNs. I-b (I8-I10) are the hairs more inferior on the labella, with the same sugar GRN population as I-a. The other neuron in this sensillum has an array of bitter receptors, some the same as previously described neurons, but also some addition GRs. The I-type have fewer bitter receptors than the S-type, but I-b has more than I-a (Freeman and Dahanukar, 2015). I-7 is left out of this description, mostly because of the inconsistency as to which population it belongs.

To further complicate matters, the distribution of physiological taste responses from what is considered one cell population are inconsistent across taste hairs to the same stimuli (Zhang et

al., 2013). Most of the differences in bitter responses across different subpopulations are likely due to different GR expression, however this is unexplained within a single population. This indicates that there are receptors that have not been identified underlying these differences, meaning there are further subpopulations within these currently characterized populations. This could also indicate a difference in stoichiometry of receptors expressed between different populations.

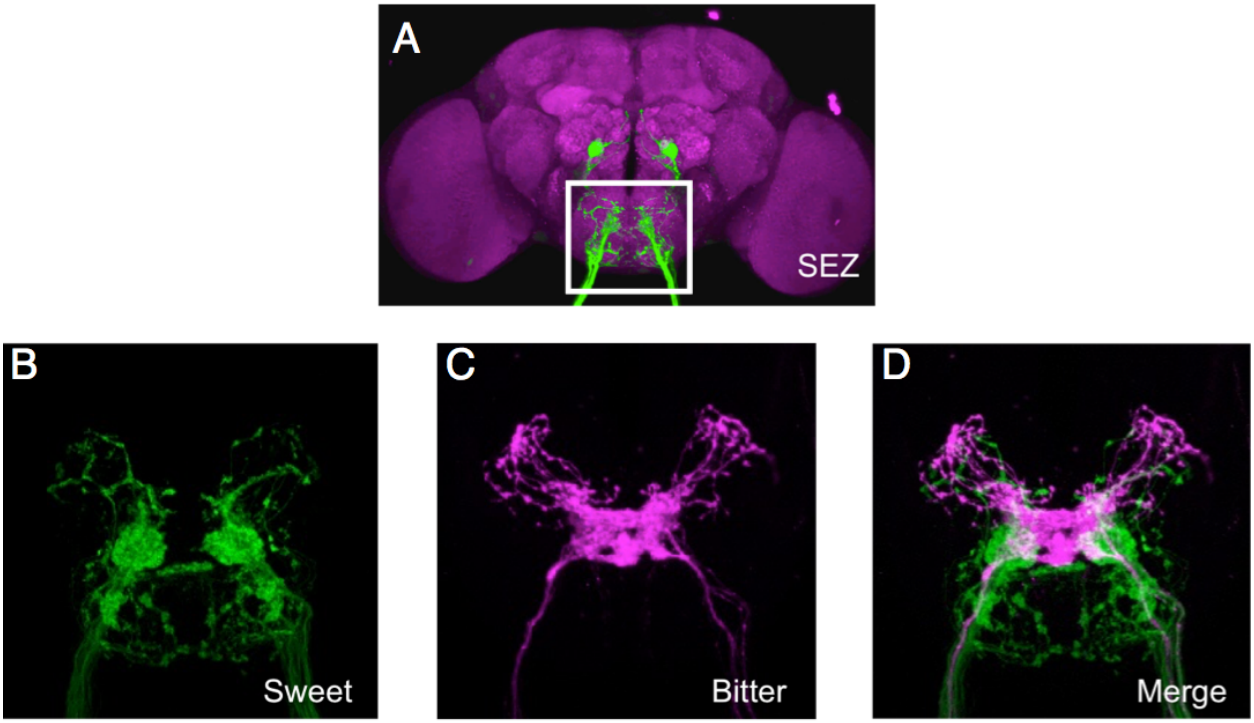

Figure 1. 4 Taste projection segregation by modality
(A) An adult fly brain, showing taste projections localized to taste center known as the subesophageal zone (SEZ). (B) SEZ zoom shows sweet neuron projections labelled by Gr5a-LexA/lexAop-GFP (green) and (C) bitter projections expressed by Gr66a-Gal4 driving UAS-dsRed (magenta). (D) Merge shows segregated, yet interacting labellar projections by modality (from LeDue, 2016).

1.1.4 Adult neural circuitry of taste

GRNs detecting a single modality are distributed over the different taste organs of the fly, and the projections are sent to the SEZ (Figure 1.4). These projections are segregated by how deep or superficial they are, as well as where they lie on the anterior-posterior plane. Depending

on where the projections are coming from on the body, they have characteristic morphologies and target areas that are recognizable to indicate body placement (Wang et al., 2004; Kwan et al., 2014). This suggests that the same GRN population could have different behavioral phenotypes depending on which body part is making contact with the tastant. The leg projections arborize in the most posterior area of the SEZ, while labellar GRNs project more medially, and pharyngeal GRNs project to the most anterior zone (Wang et al., 2004).

In addition to the segregation of gustatory organs, a segregation of taste modality in each taste organ is also observed (Figure 1.4). When looking at taste projections from the labellum, sweet and bitter GRNs are distinct, suggesting independent functional circuits for each (Wang et al., 2004; Thorne et al., 2004). Sweet GRNs presumably excite circuits that initiate acceptance behavior, while the bitter circuit drives rejection behavior. Interestingly, the water GRN projections partially overlap with the sugar GRNs, both of which drive feeding behavior (Inoshita and Tanimura, 2005). To further understand these circuits, it is important to point out the interaction between the sweet and bitter neural net. Rejection behavior can often be understood as an inhibition of acceptance behavior. Bitter GRNs project to GABAergic interneurons that arborized onto the sweet GRN to reduce activity, thus inhibiting acceptance behavior (Chu et al., 2014).

These hard-wired circuits are the main networks that drive the feeding choices of the fly. The circuits can further be modulated with starvation and deprivation of specific nutrients to change the strength of different components, affecting behavior (Inagaki et al., 2014; LeDue et al., 2016). As a fly is starved and becomes more desperate for food, it becomes more willing to accept caloric substances that are laced with bitter compounds. Additionally, a starved fly's neuronal activity in bitter cells is reduced, driving the acceptance behavior in this high-risk state

(Inagaki et al., 2014). This interaction is mediated by neuropeptides that control reciprocal changes in sweet and bitter communications (Inagaki et al., 2014). Additionally, octopaminergic neurons downstream of bitter GRNs in a ventrolateral cluster, called OA-VL, have been shown to be activated in a fed state when it is important for the fly to avoid toxicity. The activity of these neurons is reduced in a starved fly to depotentiate bitter taste and allow the fly to accept necessary calories in desperate times (LeDue et al., 2016).

Much is known about the sensory neurons in the gustatory system, but recent interest in higher order neurons is emerging, as little is known in the downstream circuitry. The first second-order gustatory neurons were characterized by Kain and Dahanukar (2015). Found to be downstream of the sugar GRNs, they were named second-order sweet gustatory projection neurons (sGPNs), and appear responsible for promoting feeding behavior. sGPNs project to the antennal mechanosensory and motor center (AMMC) and are modulated by starvation (Kain and Dahanukar, 2015). Another pair of bilateral gustatory second-order neurons, called G2N-1, were found to also be downstream of sugar GRNs (Miyazaki et al., 2015). These neurons also innervate the AMMC, indicating this area to be a novel processing center for sweet taste (Kain and Dahanukar, 2015; Miyazaki et al., 2015). Understanding downstream circuitry of the gustatory system is crucial to comprehending the complete interaction with a flies' internal state and how it chooses to interact with its environment.

1.2 The fly olfactory system

It is difficult to understand the taste system of the fly without also mentioning smell. The olfactory and gustatory systems of the fly are intimately linked and contribute to decisions made about acceptance or rejection of foods. To understand the circuitry of the gustatory system, it is valuable to compare against the understanding of the olfactory system. With more being

understood about the olfactory circuitry, and olfactory receptor (OR) genes displaying some sequence homology to GRs, it is extremely important to dissect and compare the two systems (Scott et al., 2001; Robertson et al., 2003).

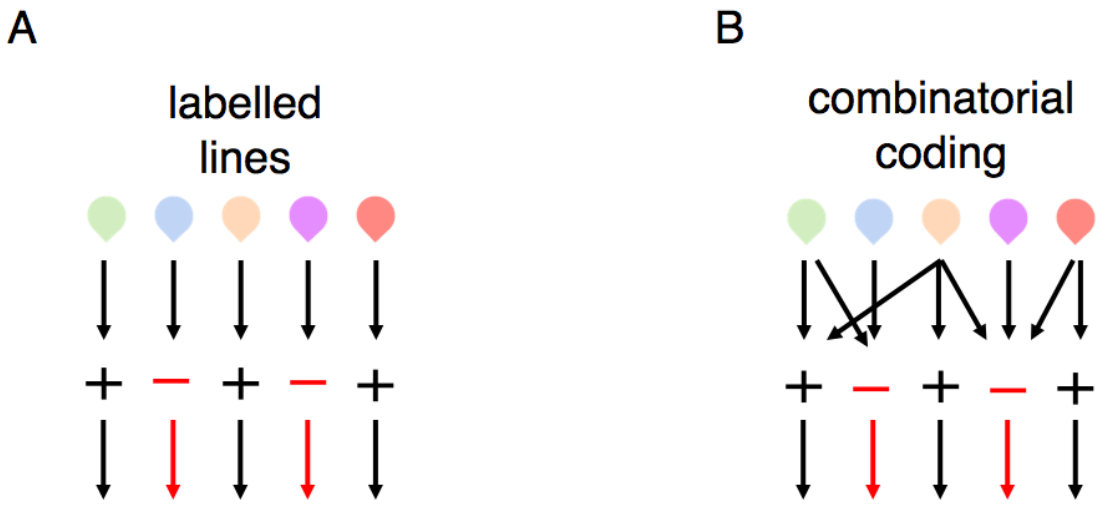

Figure 1. 5 Neural network coding in the gustatory and olfactory system
The gustatory and olfactory system differ in the way they send information to the brain. (A) The gustatory system is thought to use labelled lines coding where activation of one GRN informs an area of the brain of a binary response to drive a behavior. This allows for a simple response to many tastants (B) The olfactory system uses a combination of different ORNs to inform an assortment of glomeruli on what behavior is appropriate. This allows for a complex discrimination of odors with a relatively small number of ORNs.

1.2.1 Anatomy of olfactory network

The fly is able to smell on two independent areas of its body, the maxillary palps, found on the proboscis, and the antennae. These organs are littered with ORNs that house the different ORs, which appear structurally similar to vertebrate ORNs (Vosshall et al., 1999; Vosshall and Stocker, 2007). Similar to the gustatory organs, these ORNs reside in different sensilla distributed over the olfactory organs (Couto et al., 2005). Each olfactory sensillum contains 1-4 ORNs with an individual ORN population only expressing one OR, in addition to Orco, a member of the OR family ubiquitously expressed in all OR-expressing ORNs (Couto et al.,

2005; Vosshall and Stocker, 2007). This is different from the GRNs as these neurons only contain a single receptor that determines odor tuning, however many molecules can bind a receptor, depending on receptor specificity. These neurons send their axon projections into the brain and arborize in the antennal lobe (AL) (Scott et al., 2001). With 50-60 OR genes, this allows the animal to distinguish between many different smells (Vosshall and Stocker, 2007). Each ORN expresses a given OR and projects to a single neuropil area called a glomerulus (Scott et al., 2001; Vosshall and Stocker, 2007). This allows each odor to excite a unique assortment of glomeruli, eliciting a distinct behavior depending on the pattern of cells activated. A subset of ORNs do not express ORs, but instead express an alternative family of receptors related to ionotropic glutamate receptors (IRs). These, like ORs, are found to be localized in the dendrites of ORNs and confer responses to odorants when expressed ectopically (Croset et al., 2010). IRs were originally thought to be solely olfactory receptors as they are present in many ORNs, however are now thought to be responsible for identifying many different environmental stimuli (Croset et al., 2010). Some IRs found in GRNs distributed over different taste organs have been suggested to be responsible for sensing stimuli that GRs cannot (Joseph and Carlson, 2015).

The most important quality of comparing the gustatory and olfactory system in the fly is in how the systems are organized. The gustatory system is considered as a labelled lines model where one GRN is activated, projecting to one area of the brain, driving one behavior (Harris et al., 2015; Figure 1.5). Conversely, olfaction is organized in a combinatorial coding fashion. This allows odors to activate many ORNs, projecting to a set of glomeruli, wherein the assortment of glomeruli that are activated drive the behavior (Kundu et al., 2016; Figure 1.5). When more than one GRN type is activated, for instance the sugar and bitter populations, one GRN class will dominate in a dose dependent fashion to drive the behavior. When more than one ORN type is

activated, it is the combination of activated glomeruli that work in conjunction to drive behavior (Kundu et al., 2016; Vosshall and Stocker, 2007). This allows the fly to discriminate many more odorants than the number of receptors, as well as more dynamic behaviors attributed to these different odors. This makes the taste system seem more simplistic as it propagates binary behavioral outputs, reflecting what is assumed to be found in the neural network. When discussing whether the global flavor of a substance is appetitive or not, this is including both taste, texture, and smell. Not only do these two senses work in conjunction to drive behavior on a peripheral level, they are also presumably interconnected in their neural network within the brain (Scott et al., 2001).

1.3 Glutamate in the fly central nervous system

Glutamatergic neurotransmission has been mostly studied at the neuromuscular junction (NMJ). A map of glutamatergic neurons in the brain exists, but functional characterization of these neurons is lacking (Daniels et al., 2008). It is known through antibody staining for the *Drosophila* vesicular glutamate transporter (DVGLUT), that glutamatergic neurons are present in the optic lobe, the central complex, AL, and the SEZ (Daniels et al., 2008).

It has been shown that glutamate acts as an inhibitory neurotransmitter (NT) in projection neurons, local neurons, and the interneurons found in the AL of the adult olfactory system (Liu and Wilson, 2013; Berck et al., 2016). Glutamatergic neurons have also been identified in the gustatory sensory system, found in neurons of the legs, wings, and the labellum, but there has only been one reported case of glutamate possibly acting in the gustatory sensory system (Mahr and Aberle, 2006; Kallman et al., 2015). A subset of $ppk23^{+}$, $ppk25^{+}$ neurons, on the forelegs has been recently shown to be responsible for a neuronal population that responds to female pheromones (F cells), found on the virgin females' cuticle (Clowney et al., 2015; Kallman et al.,

2015). These "F cells" are VGLUT^{+} and drive courtship behavior. The male pheromones found on the male cuticle activate "M cells", which activate downstream inhibitory neurons to halt courtship behavior (Kallman et al., 2015). A well-defined map of cholinergic neurons in the CNS exists and continues to grow, however much is still unknown about what roles are played by the less prevalent glutamatergic neurons in the CNS play.

Glutamate can activate G-protein coupled metabotropic receptors (mGluRs). mGluRs can be found in the SEZ of both the larvae and the adult fly, although much of what these receptors regulate downstream is unknown (Ramaekers et al., 2001). It is important to note that there are motor neurons (MNs) in the SEZ responsible for driving PER that are generally positive for glutamate and can be difficult to tease apart from CNS neurons of interest (Rajashekhar and Singh, 1994b; McKellar, 2016).

1.4 Pheromone taste in the periphery

Courtship in *Drosophila* has been extensively studied and involves many facets, each defined as distinct behavioral phenotypes demonstrated by the male. Beginning with assuming close proximity to the female, chasing her, touching her abdomen with his foreleg, extending a single wing to produce vibrations resulting in a song that consists of many attempts to seduce her, licking her ovipositor with his labellum, and ultimately mounting her to perform copulation (Hall, 1994). These series of foreplay steps ascend in this very reliable sequence and can idle in repetition or retreat back to step one at any time. This happens if the complex actions are not performed up to the females' standards by the male, as well as counteractive sensory stimuli during the multiple sensory reliant steps (Thistle et al., 2012). The initiation and progression of these steps has been shown to be regulated by the different pheromones present.

The pheromones found on the cuticle of the male and female fly are a major sensory input that drives courtship behavior. The female pheromones 7,11-heptacosadiene (7,11-HD) and 7,11-nonacosadiene (7,11-ND) are found on the virgin female cuticle and are able to excite the male to drive sustained visual pursuit of the courtship target (Kallman et al., 2015). The male pheromones 7-tricosene (7-T) and cis-vaccenyl acetate (c-VA) are found on the male cuticle, and are transferred onto the female post copulation (Billeter et al., 2009). These long-chain cuticular hydrocarbons (CHCs) are manufactured in the adult fly's oenocytes, and cVA is synthesized in the ejaculatory bulb of the male fly (Ferveur, 2005). Without oenocytes, male flies are unable to evoke normal courtship behavior, indicating the necessity of CHCs (Billeter et al., 2009). The CHCs coat the cuticle and generally do not dissipate, however can be scattered when the fly moves and vibrates wings. This allows a transfer of these pheromones during the courtship ritual, and most importantly copulation, to further give information as to whether the female is mated or not (Ferveur, 2005).

In addition to the distinction of differing CHCs, the circuitry inside the fly brain also coordinates mating decisions. Just as in the mammalian brain, sexual dimorphism in neural circuitry is observed (Goodwin et al., 2000). *Fruitless* (fru) is a gene that is responsible for constructing a neural network of only a few hundred neurons that control sex-specific behaviors in the fly (Goodwin et al., 2000). Depending on where this gene is spliced out, different steps of the courtship ritual will be effected, indicating different components of the neural network to be responsible for different behavioral phenotypes (Goodwin et al., 2000). The fru^{+} network has been shown to be synaptically connected and co-localized to different taste neurons in the periphery that respond to different pheromones (Thistle et al., 2012; Toda et al., 2012; Kallman et al., 2015). Olfaction and taste work in conjunction for a normal courtship routine, as both long

and short range mating initiation take place. Arguably, taste plays a primary part in the final steps of courting and exactly how or why each step is in place still remains unknown.

1.4.1 Pheromone detection on the legs

As previously stated, one of the first steps in the male courtship initiation is tapping the female cuticle, which presumably allows tasting of her CHC composition. A series of pickpocket channel positive GRNs (ppk25^{+} and ppk23^{+}) on the legs have been shown to be responsive to pheromones and effect courtship behavior when genetically manipulated (Thistle et al., 2012; Toda et al., 2012; Lu et al., 2012; Kallman et al., 2015).

When the *ppk23* gene is mutated (Δ*ppk23*) male flies fail to initiate any courtship toward females, and vigorous male-male courting is observed (Lu et al., 2012; Thistle et al., 2012; Toda et al., 2012). Specifically, the number of single wing extensions is increased in male-male courting with Δ*ppk23* flies, as well as a constant chaining conga line resulting from males attempting to serially mount each other (Thistle et al., 2012). These defects can be rescued with a *ppk23* transgene (Thistle et al., 2012). Interestingly, this phenotype seems to be olfactory dependent as mutants lacking antennae show a complete loss of male-male courting (Thistle et al., 2012). When flies, male or female, are perfumed with aphrodisiac female CHCs Δ*ppk23* males court target flies significantly less than wildtype males, indicating a taste role for the ppk23 channel (Lu et al., 2012; Thistle et al., 2012).

Instead of completely deleting the gene, fly genetics also allows the ability to acutely silence the cell population that the channel is found in. ppk23^{+} cells have been shown to be responsive to female pheromones and when silenced decrease male-female courtship and increased male-male courtship (Lu et al., 2012; Thistle et al., 2012; Toda et al., 2012). ppk23^{+} cells are found on the male and female forelegs, with double the number of neurons being found

on the male, as well as sexually dimorphic arborizations from the leg (Lu et al., 2012; Thistle et al., 2012; Toda et al., 2012). When the fru^+ neuronal population is relieved from a silenced $ppk23^+$ population, allowing $ppk23^+/fru^+$ neurons to still remain active, all defects in courtship are lost (Thistle et al., 2012). This indicates that the ppk23-dependent courtship phenotypes are due to expression in the legs, specifically those that overlap with fru^+ neurons (Thistle et al., 2012; Toda et al., 2012).

When $ppk23^+$ cells are activated through a temperature gated cation channel in males, normal courtship is observed toward females lacking or containing oenocytes, but not towards other males (Thistle et al., 2012). This suggests that the roll of these neurons are to suppress male-male courting and promote male-female courting. However, this is contradicted by another study where activation of the $ppk23^+/fru^+$ population drove male-male courtship, arguing this activation replicated a stimulation of aphrodisiac CHCs (Toda et al., 2012). This seems to be resolved by Kallman et al., who explains that the legs contain two separate neuron populations contributing to behavior: F cell activation ($ppk23^+/DVGLUT^+$) promotes male-female courting, whereas M cell ($ppk23^+$- $ppk25^+$) activation inhibits male-female courting (2015).

When a mix of CHCs were used to stimulate the leg taste bristles, ppk23 projections in the brain increased in calcium, indicating a response of the cells through G-CaMP, whereas no response was observed to sucrose, salt, or bitter compounds (Thistle et al., 2012). When stimulating a single bristle on the legs, containing two $ppk23^+$ cells, with individual CHCs specificity for each cell was found. These F-cells and M-cells previously mentioned indicate sex-specific responses involved in sex identification that continue downstream, observed in a calcium sensor series (Thistle et al., 2012; Kallman et al., 2015). This communication from one

cell to another in this fru^+ network can be manipulated or halted at any point with the ablation or silencing of any neuron population, starting at these sensory cells (Kallman et al., 2015).

Understanding physiology in brain projections gives information about specific neuron populations in a taste organ; however, it is also valuable to observe the physiology of whole bristles housing multiple neurons to tease apart unique bristle identity within one organ. When individual taste bristles housing $ppk23^+$ neurons on the leg were stimulated with 7,11-HD, large spike patterns were observed. However, when the same bristles were stimulated with sugar, water, and salt, no significant spike pattern could be interpreted, indicating bristle specificity to pheromones (Toda et al., 2012). Conversely, bristles that did not contain $ppk23^+$ neurons do not show responses to 7,11-HD but do to all other tastants (Toda et al., 2012).

A slew of additional GRs and channels are thought to contribute to pheromone sensing, although little is known about them. Gr32a and Gr33a are proposed to be involved with pheromone sensing as they mediate male-male repulsion (Thistle et al., 2012; Moon et al., 2009; Clowney et al., 2015). Gr68a, Gr39a, and ppk25 have all been proposed to be involved in male-female attraction (Thistle et al., 2012; Clowney et al., 2015).

1.4.2 Pheromone detection on the proboscis

Much less is known about how the GRNs in the proboscis contribute to courtship or pheromone detection. ppk23 is expressed in the same number of neurons in the labellum of males and females, however unlike in the legs, $ppk23^+$ neurons do not overlap with fru^+ neurons (Thistle et al., 2012; Toda et al., 2012). Additionally, ppk25 is not expressed in the proboscis, indicating that labellar $ppk23^+$ neurons are unlikely to have properties of the F cells on the legs, although they could behave like M cells (Starostina et al., 2012). Curiously, some $ppk23^+$

neurons overlap with gr66a^{+} cells in the proboscis, but the functional relevance of this overlap is unknown (Thistle et al., 2012).

Calcium responses have been observed in ppk23^{+} labellar projections to a mix of CHCs applied to the proboscis, however the response strength is low compared to that found in the legs (Thistle et al., 2012). Moreover, there is no evidence of sexual dimorphism in these responses.

1.5 Salt taste

Salt is one of the five primary taste modalities in humans, and is also an important gustatory signal in insects. Salt is a necessary nutrient for survival and its balance is important for cell homeostasis in animals, with the gustatory system being the main sensory modality able to recognize it in the environment (Liu et al., 2003b; Contreras and Lundy, 2000). Despite the amount of work done, the exact receptors, neuronal populations, and behavioral drive behind this compound is largely enigmatic. Salt drives a bipolar behavioral response that is concentration dependent (Fujishiro et al., 1984; Wieczorek and Wolff, 1989; Lemon and Katz, 2007). Even defining 'high' and 'low' salt is debatable, with low salt ranging from 50mM-200mM and high salt >200mM, although it is thought that a 100mM concentration will activate both high and low salt pathways (Hiroi et al., 2004). Publications reporting salt responses in flies often implicate pickpocket genes coding for DEG and ENaC, the same family responsible for low salt detection in mammals (Liu et al., 2003b; Alves et al., 2014; Chandrashekar et al., 2010). However, the ENaC nonspecific antagonist amiloride does not completely eliminate salt taste, suggesting that this channel is not the only responsible salt sensor (Liu et al., 2003b). Understanding this bimodal sensory switch on a neuronal level has been a long evolving area of research in the fruit fly.

1.5.1 Larval salt taste

Larvae can both sense salt and discriminate between different salts, indicating a significant dedication of the gustatory system to salt sensing (Liu et al., 2003b). Larvae have a single gustatory organ, called the terminal organ (TO), which houses around 30-40 GRNs, making it much more simple than the adult fly taste system. Both ppk11^{+} and ppk19^{+} neurons were found in the TO to be responsible for low salt detection. Flies with disrupted ppk11^{+} cells still had intact high salt detection, however flies with disrupted ppk19^{+} neurons had reduced high salt responses (Liu et al., 2003b). It's possible that some channels contribute to both high and low pathways.

The *serrano* (*sano)* gene locus encodes an apparent cytoplasmic protein and when mutated in the TO, leads to a loss of avoidance to high salt (Alves et al., 2014). Attraction to low salt and aversion to bitter compounds is still intact in these Δ*sano* flies, indicting this protein to be expressed in cells responsible for high salt detection only. Δ*Gr66a* shows a similar, but less severe effect, indicating the bitter population also plays a role in high salt detection (Alves et al., 2014). Interestingly, sano^{+} cell bodies increase in calcium activity, indicating a sensory response, to a high salt stimulus only if both *sano* and *ppk19* are present (Alves et al., 2014). This supplies evidence that Sano is working in the ppk19^{+} population to sense high salt in the larvae.

1.5.2 Adult labellum

A closer look at the understanding of how salt is coded in the labellum highlights the confusion surrounding neuron responsibility. Based on early research conducted from various labs, a model was presented by Makoto Hiroi and colleagues where S-type and L-type sensilla house four GRNs: the W cell, S cell, L1 cell, and L2 cell, responding to water, sugar, low salt, and high salt respectively (Fujishiro et al., 1984; Wieczorek and Wolff, 1989; Hiroi et al., 2002).

The I-type were then described to house just an S cell and an L2 cell, responding to sugar and low salt, and bitter and high salt, respectively (Hiroi et al., 2004). Establishing this through extracellular sensillum recordings and deciphering between neuron spike patterns, Hiroi observed that not all sensilla were equal, and one neuron can respond to more than one stimulus (2002). However, calcium imaging suggests that high salt presented to the labellum will evoke a response in both sugar and bitter cells, although the driver used to label sugar cells is not completely specific (Marella et al., 2006; Fujii et al., 2015). This, along with a series of papers showing additional novel responses, forced a remapping of the labellum where sensilla were put into five smaller groups based on neuron type (Freeman and Dahanukar, 2015). The model presumes all bitter cells respond to high salt, although whether the response was due to bitter receptors or a novel receptor was unknown. Low salt responses were suggested to occur in all sugar cells, as well as a newly identified low salt cell expressing *Ir76b* and found in the L-type sensilla (Zhang et al., 2013). Although most papers have hinted that salt responses cannot be isolated to a specific sensillum, neuron, or receptor, salt taste coding in the labellum remains opaque. Additionally, because the combination of physiology found throughout the literature does not necessarily match the neuron populations grouped in these five collections, indications of unknown salt responsive populations exist.

Although Ir76b^{+} cells have been presented as dedicated salt sensors, Ir76b is also necessary for the detection of amino acids and polyamines (Zhang et al., 2013; Ganguly et al., 2017; Hussain et al., 2016). It is possible that Ir76b^{+} neurons in different taste organs are responsible for different neural circuits, and thus behaviors. For example, salt elicits a response from Ir76b neurons in the labellum, amino acid elicits a response in the legs, and taste pegs

respond strongly to behavioral relevant polyamine concentrations (Zhang et al., 2013; Ganguly et al., 2017; Hussain et al., 2016).

Additional reports suggest other populations of GRNs responding to salt. ppk11^{+} neurons are found in the labellum, labelling more than one neuron per taste hair, and silencing of these neurons reduces high salt avoidance (Liu et al., 2003b). Moreover, a group of doublet neurons, *dpr*$^{+}$ cells, found in some unspecified places of the labellum, have been shown to play a role in high salt detection (Nakamura et al., 2002). This *dpr* gene encodes a transmembrane protein with an Ig repeat that is of unknown function, but has the possibility to be a receptor (Nakamura et al., 2002).

Presently, the picture of fly salt taste is obscure and confusing. Most of this is due to assumptions made between different experiments found in the literature that are not necessarily answering the same questions. Adult flies taste on multiple areas of their bodies, and we are often not able to restrict genetic lines to specific taste organs, so it is difficult to tease apart different responses from different organs. It is crucial to understand the circuitry from distinct body areas as they are segregated, only then can we obtain an understanding of the interaction between each organ's GRN population and how they contribute to driving behavior.

1.5.3 Interaction between salt gustatory cues drives behavior in animals

It is known that mated females are more attracted to salt than virgin females or males (Walker et al., 2015). This is unsurprising as similar behavioral changes are seen in mammals, including humans (Faas et al., 2009; Clarke and Bernstein, 2001). In flies, this appears to be driven by Ir76b^{+} cells, as increased PER to low salt is lost when these neurons are silenced (Walker et al., 2015). The change in salt sensitivity happens when Sex Peptide (SP) is transported through seminal fluid to the female and activates Sex Peptide Sensory Neurons

(SPSNs) in the reproductive tract, acting on the canonical postmating circuitry (Walker et al., 2015). It is still unknown whether this increase happens at a sensory neuron level, or if it is further downstream in the system. It also remains unknown exactly what the functional reasons are for this change, but flies fed on a salt diet after copulation lay more eggs than flies deprived of salt; however, the viability of the eggs laid does not change (Walker et al., 2015). It is proposed that a female may have an increased appetite because ions are needed to maintain osmotic balance during egg production, as well as salt could act as a phagostimulatory factor in flies to increase their appetite in order to increase healthy egg production (Walker et al., 2015). As previously stated, Ir76b^{+} cells have also been shown to be necessary for polyamine detection, a compound that is also preferred for egg laying. When Ir76b^{+} cells are silenced, the preference for egg laying on a polyamine rich medium is also lost (Hussain et al., 2016).

As discussed, the attraction and aversion of salt based on concentration is thought to be mediated by two independent pathways, with both cell populations contributing to normal behavior. Mammals show an increased appetite for low NaCl when they are salt deprived, as well as increased activity in the ENaC pathway (Chandrashekar et al., 2010). ENaC knockout mice lose this attraction post deprivation while their high salt aversion remains intact, indicating necessity for the low salt pathway. This ENaC circuitry is specifically tuned to sodium salt, as where the high salt circuitry is cation non-specific (Chandrashekar et al., 2010). This physiology is likely a survival technique as an aversive pathway should be more promiscuous in its ability to be activated, in an attempt to avoid toxins. Whereas the appetitive pathway needs to be more selective as to be careful to ingest only what is nutritious.

1.5.4 Comparisons between insect and mammalian salt taste circuit

The mammalian tongue is organized slightly differently than any taste organ of the fly. The mammalian tongue houses taste receptor cells (TRCs) and each TRC is thought to respond to one of the five basic tastes: sweet, sour, bitter, salt, and savory (Oka et al., 2013; Chandrashekar et al., 2010). This neural network is organized in the same labeled lines model as the fly, where each TRC population corresponds to one of the basic modalities, with an animal being able to taste multiple modalities at once. However, recent research has shown that TRCs are able to respond to more than one stimulus, as well as recruit other TRC pathways to effectively drive behavior (Oka et al., 2013). For example, bitter sensing TRCs show an additional response to high salt. Similarly, sour sensing TRCs also show a response to high salt (Oka et al., 2013). It is unknown whether the cross talk between these pathways is due to a receptor on the cell or possible signaling between the populations. Additionally, double mutants of these cell populations which leave the low salt ENaC pathway intact show an attraction to high salt (Oka et al., 2013). The labeled lines model of taste in mammals is therefore starting to be questioned, as rodent bitter TRCs are equally as responsive to intermediate salt concentrations, but rats are still able to discriminate between these compounds (Lemon and Katz, 2007). With both insects and mammals, the gustatory field is becoming more convinced that the labeled lines model that is of the current dogma may need to be revisited, as more research shows possible combinatorial properties within the networks (Reiter et al., 2015; de Araujo et al., 2012).

ENaC have been discussed as the main low sodium salt sensor in mammals, driving appetitive behavior (Chandrashekar et al., 2010). ENaCs are specifically tuned to sodium salt, and can sense concentrations from 10mM-120mM (Hanukoglu and Hanukoglu, 2016).

Interestingly, high salt pathways that are not mediated by ENaCs, are not sodium specific, and can sense concentrations starting at 150mM.

1.6 Technical details

An array of different techniques are used to describe the anatomy and receptive field of sensory neurons in the fly. The Gal4/*UAS* system is a critical tool for genetic manipulation found in most fly research. The use of genetically coded calcium indicators (GECIs) are widely used in animal research, and GCaMP has been specifically adapted for use in flies.

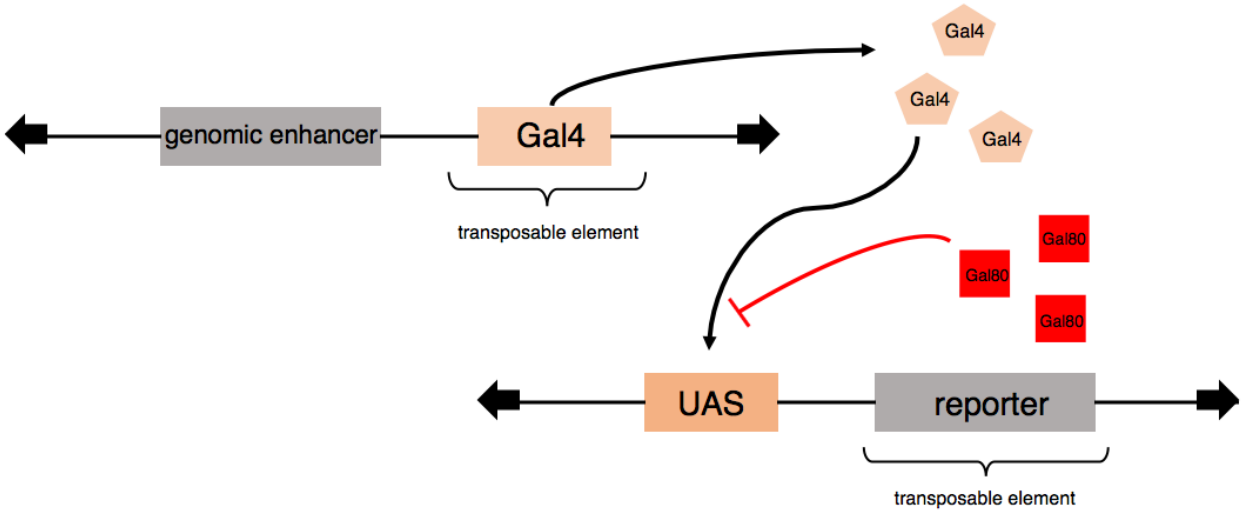

Figure 1. 6 Drosophila Gal4/*UAS* system
One transgene contains a yeast transcription factor Gal4 that is expressed under the control of the intended promoter sequence of the gene of interest, labeling a group of cells. The second transgene contains an upstream activating sequence, *UAS*, that then binds the Gal4 which contains the intended insert gene of interest. *gal80* is a protein which binds to the Gal4 transcriptional activation domain, blocking the Gal4 from binding the *UAS*.

1.6.1 Gal4/*UAS* system

The Gal4 system of the fruit fly has immensely advanced the field of research not only in neuroscience, but also development, behavior, and genetics. It allows for very specific genetic manipulation and temporal resolution that has given the ability to answer important questions about where and when. It involves two transgenic animals that when crossed together result in a

genetically altered animal. One fly contains a yeast transcription factor Gal4 that is expressed under the control of the intended promoter sequence of the gene of interest, labeling a group of cells. The second fly contains an upstream activating sequence, *UAS*, that then binds the Gal4 which contains the intended insert gene of interest (Brand and Perrimon, 1993; Figure 1.6). Any gene can be coupled to the *UAS* depending on what questions about the Gal4 cell population are to be answered. This allows strict control of the *UAS* to the Gal4 promoter, restricting expression of the desired protein in the cells of particular interest (figure 1.6). Notably for neuroscience, neuronal populations can be labeled, activated, and silenced in a multitude of ways through the use of this system (Venken et al., 2011).

The Gal4 can be restricted even further using *UAS-gal80*, which binds to the Gal4 transcriptional activation domain, blocking the Gal4 from binding the *UAS* (Figure 1.6). Additionally, gal80^{ts}, is a temperature sensitive variant that can be used to repress that Gal4 at lower but not higher temperatures (Gordon and Scott, 2009). This is useful when overlapping populations exist and need to be observed independently.

The success of this binary expression system led to an additional system that allows for the same manipulations in isolation, that can be used in conjunction with the Gal4 system. The LexA/*LexAop* complex works similarly where the transcription factor, LexA activates the LexA operator, *LexAop* (Lai and Lee, 2006). This allows for both binary expression systems to be used simultaneously and independently to alter different populations of neurons at the same time, under different experimental controls.

1.6.2 GCaMP imaging

GECIs are popular tools used to record the flow of intracellular Ca^{2+} in neurons, which can be used as a proxy of action potentials (APs), and thus activity. When a cell depolarizes,

there is a flux of Ca^{2+} into the cell from both the extracellular domain and the endoplasmic reticulum causes a spike in Ca^{2+} concentration (Berridge, 1998). GECIs are used in flies to noninvasively target specific cell populations and characterize receptive fields of the populations' soma and projections *in vivo*. They can also give information about neural circuitry when stimulating one population and recording from downstream neurons.

All indicators use an adulterated green fluorescent protein (GFP) variant to construct these GECIs, with the most common and efficient being GCaMP. GCaMP is derived from the circularly permuted GFP (cpGFP) that is fused to the calcium binding protein calmodulin's (CaM) binding site M13, allowing the CaM, decorated with Ca^{2+} binding domains, to be exposed (Nakai et al., 2001). This protein construct has a low basal fluorescence, as the fluorescence is muted by the unideal cpGFP confirmation. As calcium flows into the cell, filling the binding cites on CaM, a conformational change occurs where M13 moves to close the pore of cpGFP allowing the full fluorescence to be exposed (Nakai et al., 2001). It is this dance of molecule transitions, triggered by Ca^{2+}, that allows the ability to monitor activity in a temporally relevant fashion of many cells at once.

GCaMP imaging offers cell-type specificity and is a less invasive measure of activity compared to electrophysiology. Although the specific rate of APs is unknown when using GCaMP, one AP can trigger the conformational change (Chen et al., 2013). Most importantly the cells are not damaged; not to mention, the size and density of neurons in the fly brain makes electrophysiology near impossible for deeper brain areas. This also allows for a whole population code rather than one cell 'speaking' for the whole group, although both are important. The synthetic calcium indicator OGB-1 was the favorite to GCaMP until recently, as it was faster at binding calcium and had greater photostability. However, it also needs to be injected into the

brain, reducing specificity, paired with slower decay kinetics and inefficient binding of calcium (Hendel et al., 2008). GCaMP6 has thus surpassed its synthetic counterpart as it has better binding efficiency and a higher signal-to-noise ratio (Chen et al., 2013). GCaMP6, in comparison to GCaMP3, has provided better resolution for neuron receptive fields, and has opened the door to both revisiting previously characterized populations and novel discovery of cell circuits as well as spontaneous activity.

2 Materials and Methods

2.1 Fly stocks

Flies were raised on standard cornmeal fly food at 25°C in 70% humidity and moved to room temperature upon enclosure. The following fly lines were used: *vGlut^{MI04979}-Gal4*, *Cha^{MI04508}-Gal4*, *vGlut^{MI04979}-LexA::QFAD*, and *Cha^{MI04508}- LexA::QFAD* (Diao et al., 2015); *Ir76b-Gal4* (Zhang et al., 2013); *Gr66a-LexA* known to label the bitter gustatory population, *Gr64f^{LexA}* known to label the sweet gustatory population (Miyamoto et al., 2012); *ppk23-LexA* known to label a pheromone gustatory population, and *UAS-CD8::tdTomato* (Kallman et al., 2015); *Gr66a-Gal4* known to label the bitter gustatory population, (Wang et al., 2004); *ppk28-LexA* known to label the water gustatory population*; ppk23-Gal4* known to label a pheromone gustatory population*, LexAop-Gal80* (Thistle R et al., 2012); *LexAop-GFP* (Lai and Lee, 2006); *LexAop-Flp, UAS-stop-GFP* (von Philipsborn et al., 2011); *UAS-GCaMP6f* (Chen TW et al., 2013).

2.2 Tastants

Sucrose (Sigma-Aldrich), NaCl (VWR), KCl (Sigma-Aldrich), MSG (Six Fotune) were kept as 1M stocks in ddH2O at 4°C, and diluted as needed. Lobeline hydrochloride was kept as 1.25mM stock in ddH2O at 4°C, and diluted as needed (Sigma-Aldrich). Acetic Acid was kept in a 10% solution in ddH2O at room temp and diluted as needed (Fisherbrand). 7,11-heptacosadiene (7,11-HD), 7,11-nonacosadiene (7,11-ND), and 7-tricosene (7-T) were diluted in ddH20 to desired 0.0001mg/ul as needed (Cayman Chem). Cis-vaccenyl acetate (c-VA) was diluted to stock solution of 0.01mg/ul in ethanol (EtOH), and then diluted in ddH2O as needed (Cayman Chem). All hydrocarbons stocks were kept at -20°C, diluted as needed, and stored at

4°C for up to seven days. 1% of each EtOH (UBC chemistry) and Hexanol (Sigma-Aldrich) were diluted in a mix with ddH2O and kept at 4°C for control solution.

2.3 Immunohistochemistry

Immunofluorescence protocol for labella was carried out as described (Jeong et al., 2016). Labella were dissected and fixed for 25 minutes in 4%PFA in PBS+0.2% Triton. After washing with PBST (0.2%), labella were blocked in 5% NGS diluted with PBST (0.2%) for 40 minutes. Primary antibodies were applied and incubated at 4°C overnight: chicken α-GFP (1:1000; Abcam #13970) and rabbit α-RFP (1:200; Rockland #35055) were used. After washing for 1 hour, secondaries were applied for 2 hours: goat α-chk Alexa 488 (1:200; Abcam #150169) and goat α-rabbit Alexa 647 (1:200; Life Tech #A21245). Labella were washed again for 40 minutes, placed on slides in SlowFade gold, with small coverslips as spacers, and imaged.

All images were acquired using a Leica SP5 II Confocal microscope with a 25x water immersion objective. All images were taken sequentially, z-stack step size at 2um, a line average of 2, speed of 200 Hz, and a resolution of 1024 x 1024 pixels.

2.4 Labellar neuron annotation

To annotate the expression of different markers in the labellum, each sensillum was analyzed independently over 4-8 labella. We went through each z-stack to identify how many neurons in each sensillum were positive for the different drivers, and which neurons overlapped with the respective co-labelled population. In any given sensilla, verification for the number of labelled neurons against the known population's neuron number was performed. If any other neurons were observed, they were not counted. The majority for each neuron in each sensillum was used and reported. Sensilla S0, I0, I9, and I10 were the most difficult to score as they were often missing from the prep, or more inconsistent after scoring. At times there were duplications

of specific sensilla on a labellum, in which case both sensilla were taken into account; if inconsistencies arose, the sensillum that contained the expected neuron populations was used.

2.5 GCaMP imaging

For calcium imaging experiments, female or male flies were aged from 2-10 days in groups. To prepare the flies for experiments they are briefly anesthetized using CO2, legs amputated for full access to proboscis, and placed in custom chamber suspended from their cervix. To ensure immobilization, a small drop of nail polish is applied to the back of the neck and the proboscis is pulled to extension and waxed out on both sides. A modified dental waxer was used to apply wax on each side of the chamber rim, making little contact with the feeding structure. Flies were left to recover in a humidified chamber for 1 hour. The antenna were removed from the fly and a small window of cuticle was removed from the top of the head, exposing the SEZ. Adult Hymolymph Like (AHL) buffer was immediately applied to the preparation (108 mM NaCl, 5 mM KCl, 4 mM NaHCO3, 1 mM NaH2PO4, 5 mM HEPES, 15 mM ribose). The air sacs, fat, and the esophagus were clipped and removed to allow clear visualization on the SEZ. A coverslip was used to isolate the proboscis and keep it available for stimulation of tastants. Once ready to image, AHL buffer was added that includes Mg^{2+} and Ca^{2+} (108 mM NaCl, 5 mM KCl, 4 mM NaHCO3, 1 mM NaH2PO4, 5 mM HEPES, 15 mM ribose, 2 mM Ca^{2+}, and 8.2 mM Mg^{2+}).

GCaMP6f fluorescence was observed with a Leica SP5 II Confocal microscope with a 25x water immersion objective. The relevant area of the SEZ was visualized at a zoom of 4x, at a speed of 8000 Hz, a line accumulation of 2, and resolution of 512 x 512 pixels. The pinhole was opened to 2.98 AU. For each taste stimulation, a baseline of 5 s was acquired prior to stimulation, 1 s for tastant application, and 9 s following the stimulation.

Before recording, a pulled capillary pipette was filed down to match the size of the proboscis and fit perfectly over all taste sensilla on both labellar palps. The pipette was filled with 1-2ul of a tastant and positioned a few microns away from the proboscis labellum. At 5 s a micromanipulator was used to apply the tastant to the labellum manually. Between taste stimulations of differing solutions, the pipette was washed with water. All NaCl solutions were applied in the order of increasing concentration, finishing with 1M KCl. All other solutions were randomly applied to control for potential inhibitory effects between modalities, 1% acetic acid was always applied last.

The maximum change in fluorescence (ΔF/F) was calculated using the peak intensity (average of 3 time points) minus the average intensity at baseline (10 time points), divided by the baseline. Quantification of fluorescence changes was performed in ImageJ and graphed in GraphPad Prism6.

2.6 Salt deprivation

Flies were aged for 2-5 days and then placed in deprivation vials for 48 hours. Salt satiated flies were placed on a medium that contained 1% agar, 5% sucrose, and 10mM NaCl. Salt deprived flies were placed on a 1% agar and 5% sucrose medium. Flies were kept in deprivation vials containing 5-8 flies at room temperature. Flies were imaged as described for calcium imaging after two days.

2.7 Statistical analysis

Statistical tests were performed using GraphPad Prism 6 software. For all imaging data a one-way ANOVA was done. For all salt concentrations, a Tukey's multiple comparisons test was run. For all other stimuli, a Dunnett's multiple comparisons test was done comparing all tastants to water.

3 Results

3.1 ppk23^{+} neurons, but not other GRNs, express VGLUT

Sensory neurons within a specific class are generally thought to be homogenous in terms of neurotransmitter release. Thus, the existence of VGLUT^{+} GRNs among the largely cholinergic population of neurons, raised the question of whether the GRNs releasing glutamate have a single specific identity and function. To address this question, we took advantage of the Gal4/*UAS* and LexA/*LexAop* systems to express fluorescent proteins and examine co-labelling with markers for specific GRN types: *Gr66a-LexA* (bitter cells), *Gr64f-LexA* (sugar cells), *ppk28-LexA* (water cells), *ppk23-LexA* (putative pheromone cells). *VGLUT-Gal4* (glutamate transporter) and *ChAT-Gal4* (acetylcholine synthesis enzyme) were used as a proxy to mark NT cell types in GRN populations.

First, I determined that VGLUT is expressed in one cell per sensillum of all S-type and L-type sensilla, as well as I0, I6, and I9 (Figure 3.1 and 3.5).

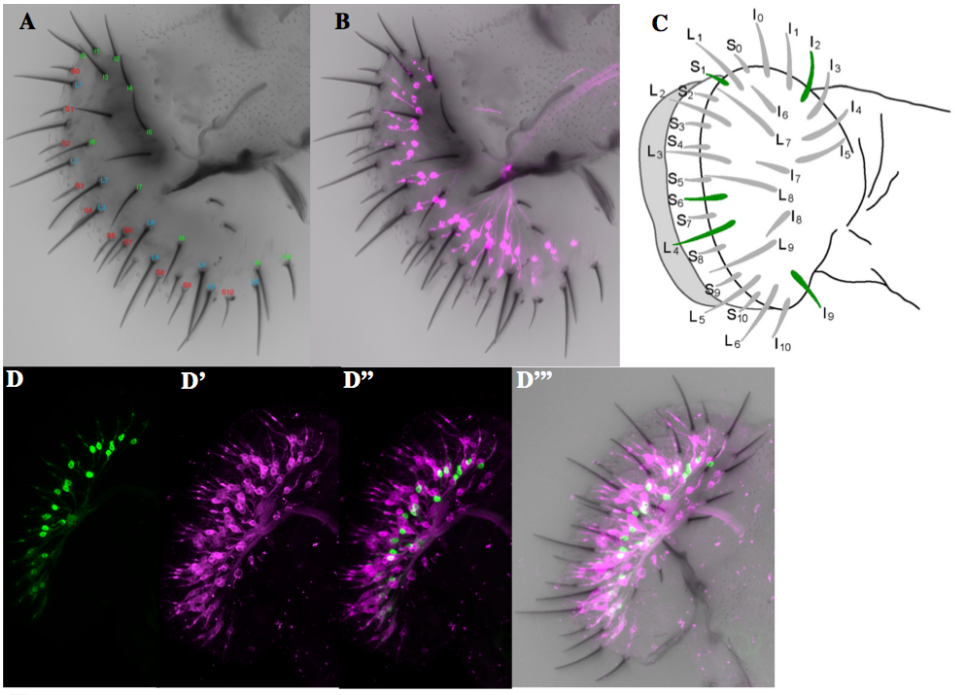
A
B
C
D
D'
D''
D'''

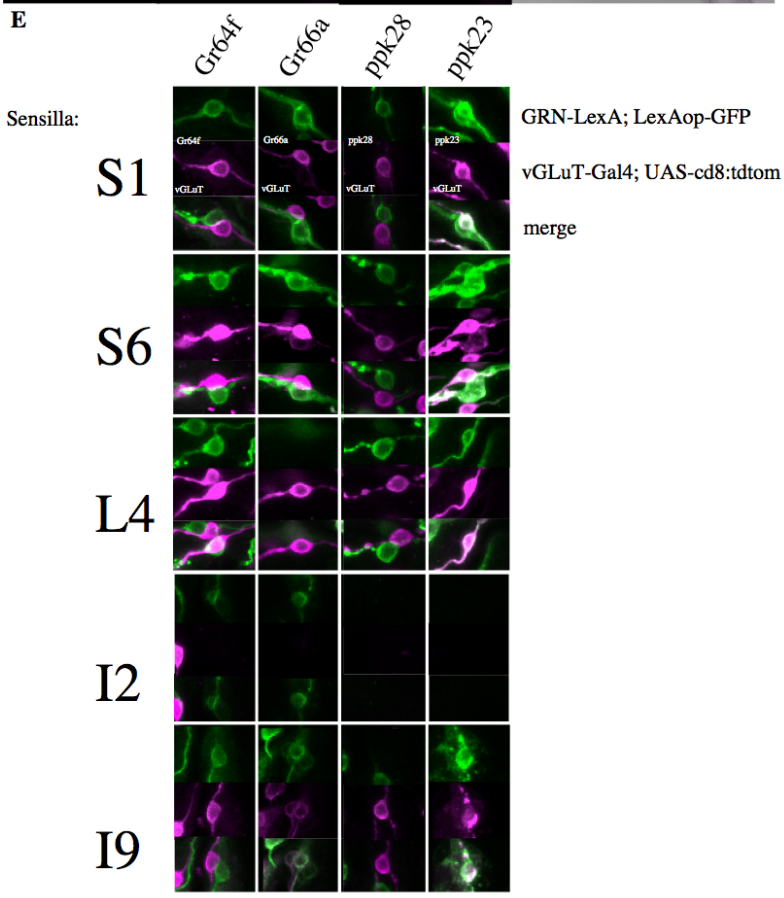
E
Gr64f
Gr66a
ppk28
ppk23
Sensilla:
S1
S6
L4
I2
I9
GRN-LexA; LexAop-GFP
vGLuT-Gal4; UAS-cd8:tdtom
merge

Figure 3.1 Glutamate and Acetylcholine in the labellum
Antibody staining of (A-D) Single labellar palp or (E) representative individual sensilla from flies expressing CD8::tdTomato (magenta) under the control of *VGLUT-Gal4*. (A) Labelled sensilla of a labellar palp with (B) VGLUT expression shown in each sensilla. (D) Flies expressing GFP (green) under the control of *VGLUT-LexA* show no overlap (D'') with (D') CD8::tdTomato under the control of *vChAT-Gal4*. (C) Cartoon of single labellum, green indicates specific sensilla, S1, S6, L4, I2, and I9 used (E) to show overlap with different GRNs. Different GRNs expressing GFP under the control of *Gr64f-LexA, Gr66a-LexA, ppk28-LexA*, and *ppk23-LexA* respectively. White arrows indicate overlap observed between GRN population and *VGLUT-Gal4* (expressing CD8:tdTomato) population. All images taken live at 25x.

Next, co-labelling VGLUT$^+$ and ChAT$^+$ populations together confirms that no cells in the labellum release both NTs (Figure 3.1). Close examination reveals that all S and L-type sensilla have three ChAT$^+$ cells and one VGLUT$^+$ cell, as where I-type have either two ChAT$^+$ cells, or one ChAT$^+$ cell and one VGLUT$^+$ cell. *VGLUT-Gal4* and *VGLUT-LexA* show complete overlap in the GRN populations that they label (not shown). We found that, as expected, most sensory neuron populations are ChAT$^+$, using acetylcholine to communicate downstream to other neurons. Moreover, we know that any population that is not VGLUT$^+$, is instead ChAT$^+$. This was true for Gr66a$^+$, Gr64f$^+$, and ppk28$^+$ GRNs as no overlap was found with these populations and VGLUT$^+$ (Figure 3.1). However, most ppk23$^+$ GRNs are VGLUT$^+$, indicating this population is unique in its use of glutamate to communicate downstream (Figure 3.1 and 3.2). Interestingly, there are some sensilla that contain more than one ppk23$^+$ neuron, mirroring what is seen in the legs (Kallman et al., 2015). It became increasingly important to analyze each sensilla independently, as not all populations within each are consistent. Figure 3.1 shows five representative sensilla examples of each GRN and glutamate populations that represent the different groups of GRN populations observed over all sensilla.

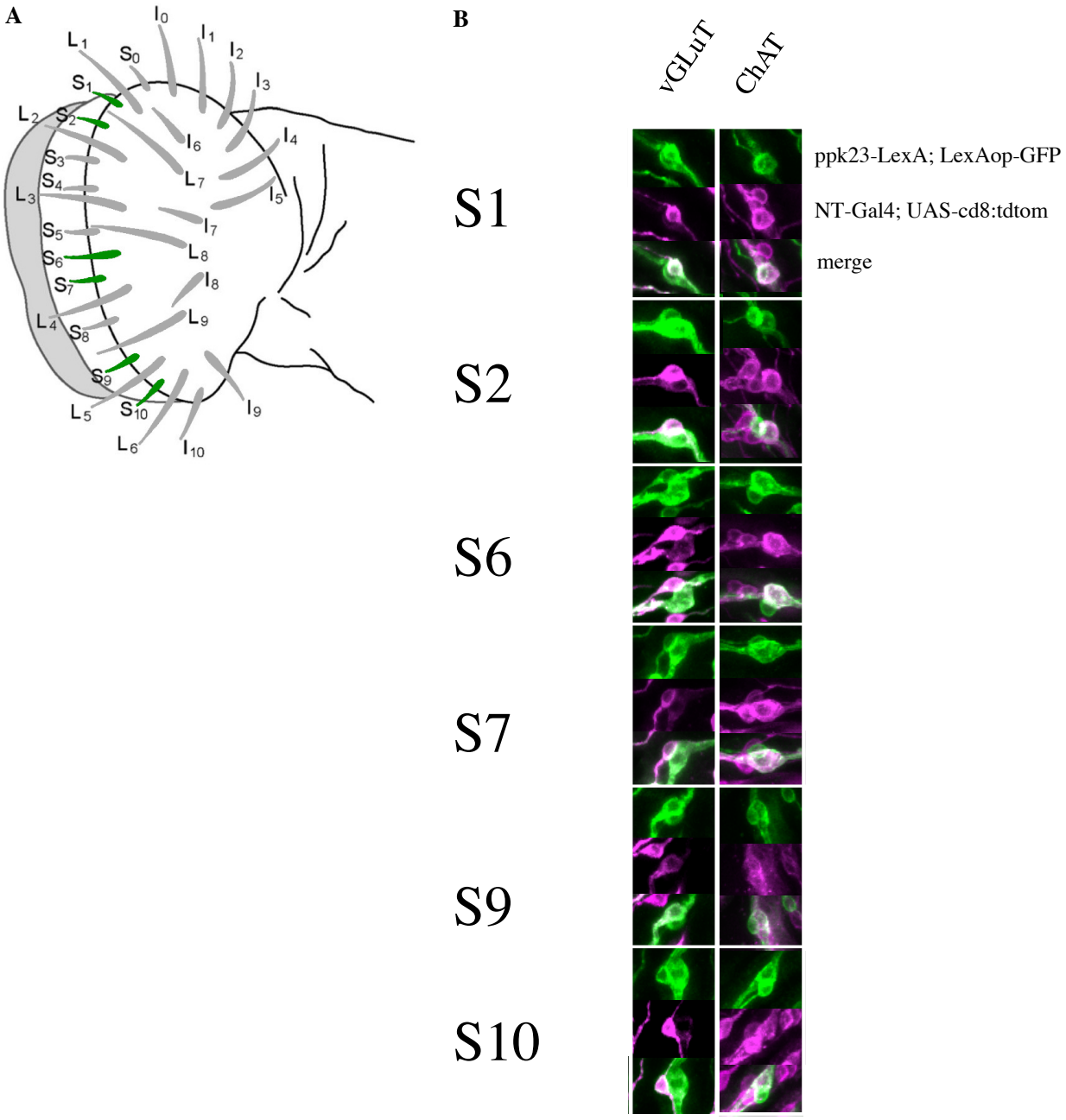

Figure 3.2 One neuron in S-type ppk23 doublets are VGLUT$^+$
(A) Cartoon of single labellum, green indicates specific sensilla, S1, S2, S6, S7, S9, and S10 that have ppk23$^+$ doublets. (B) Antibody staining of representative individual sensilla from flies expressing CD8::tdTomato (magenta) under the control of VGLUT-Gal4 or vChAT-Gal4. Co-expression of GFP (green) under the control of ppk23-LexA shows independent overlap with the two NT in each cell. All images taken live at 25x.

After scoring at least three labella for each combination of GRN marker plus *VGLUT-Gal4*, we were able to produce a map of neurons in each sensillum (Figure 3.5). Consistent with

previous reports, Gr66a^{+} bitter GRNs are present in all S-type and I-type sensilla (Weiss et al., 2011). Gr64f^{+} sugar GRNs are expressed in all S, L, and I-type sensilla (Dahanukar et al., 2007). ppk28^{+} water cells are expressed in all L type sensilla, and are only expressed in S0-S2, S6, S7, and S10 (Inoshita and Tanimura, 2005). ppk23^{+} cells are expressed in S-type sensilla as previously proposed, but we also find them in all L-type sensilla. In S1, S2, S6, S7, S9, and S10 there are two ppk23^{+} neurons, where one is small and is co-labelled with VGLUT^{+}, and one is large and co-labelled with ChAT^{+} (Figure 3.2). All ppk23^{+} cells found in L-type sensilla, and are VGLUT^{+}. ppk23^{+} cells are also found in I0, I6, and I9 and are co-labeled with VGLUT^{+}. ppk23 expression is are not found in S4 or S8, as with many GRs, but a VGLUT^{+} cell is still present. These are not the only neurons in the labellum found to be VGLUT^{+} but not ppk23^{+}, indicating a subpopulation (Figure 3.5).

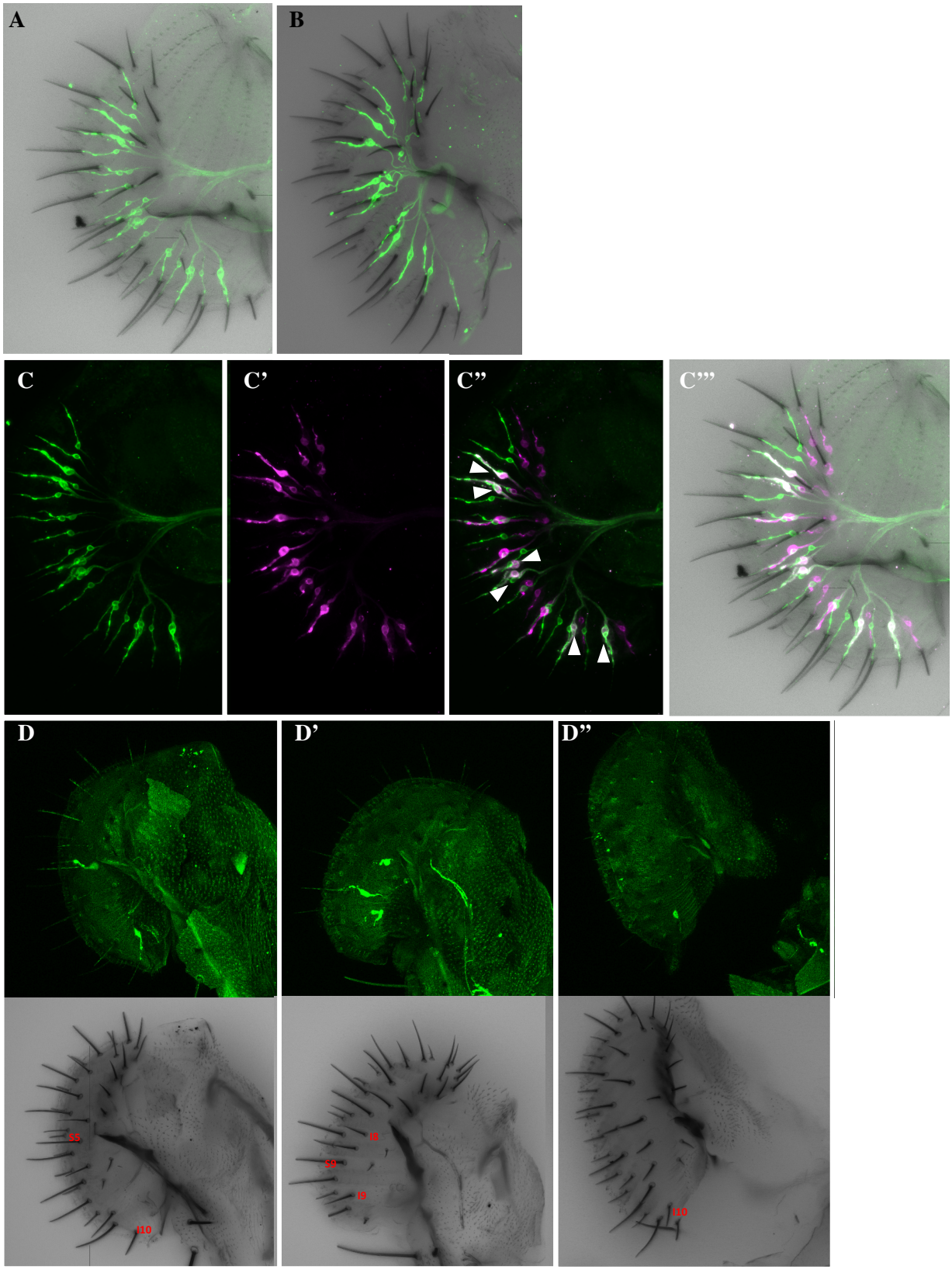
A
B
C
C'
C''
C'''
D
D'
D''
S5
I10
I8
S9
I9
I10

Figure 3.3 ppk23 overlaps with Gr66a in six sensilla
Antibody staining of (A-B) Single labellar palp expressing GFP (green) under the control of (A) ppk23-lexA and (B) Gr66a-lexA. (C) Labellum showing GFP under the control of ppk23-LexA and (C') CD8::tdTomato under the control of Gr66a-gal4 shows some overlap (C'') indicated by white arrows. (D) Live labella with GFP expression under the control of Gr66a-Gal4/VGLUT-lexA; lexAop-Flp/UAS-stop-GFP paired with bright field images to indicate sensilla type. GFP expression indicates inconsistent Gr66a$^+$ and VGLUT$^+$ neurons. All images taken at 25x.

3.2 ppk23 overlaps with Gr66a in six sensilla

We became increasingly interested with the second neuron found in the six sensilla labelled by *ppk23-lexA* that did not express VGLUT$^+$, but instead ChAT$^+$. By co-expressing ppk23-lexA/*LexAop*-GFP and Gr66a-Gal4/*UAS*-cd8:tdtom, we observed overlap in six cells found in: S1, S2, S6, S7, S9, and S10 (Figure 3.3). These ppk23$^+$/Gr66a$^+$ cells express ChAT$^+$ and appear to account for the second ppk23$^+$ neuron found in the doublet (Figure 3.3 and Figure 3.5).

3.3 Gr66a$^+$ cells do not reliably express VGLUT

Although all of the neurons co-expressing ppk23 and gr66a appear to be ChAT$^+$, we next wanted to verify that there is no Gr66a expression within the VGLUT$^+$ population of ppk23 neurons. Additionally, the Gr66a$^+$ population shows full overlap with ChAT$^+$ and appears to be cholinergic, it also appears to have inconsistent expression of VGLUT$^+$ (Figure 3.1). When a Gr66a$^+$ cell appears to be co-expressed with VGLUT$^+$ cells, there appears to be more than one VGLUT$^+$ neuron in that sensillum (Figure 3.2). We know that there is only one VGLUT$^+$ cell in each sensillum.

To address these questions, I took advantage of the FLPout system. This system uses site directed recombination to manipulate the two binary systems, restricting expression only to where overlap exists (del Valle Rodriguez et al., 2013). When restricting the Gr66a$^+$ population to only express GFP in neurons that also contain VGLUT$^+$ cells, very little GFP expression is observed in the labellum (Figure 3.3). When looking between three labella, 1-3 neurons fluoresce

GFP and the expression is inconsistently scattered over many sensilla. This indicates that there may be sporadic overlap between Gr66a and VGLUT, but is likely not biologically relevant.

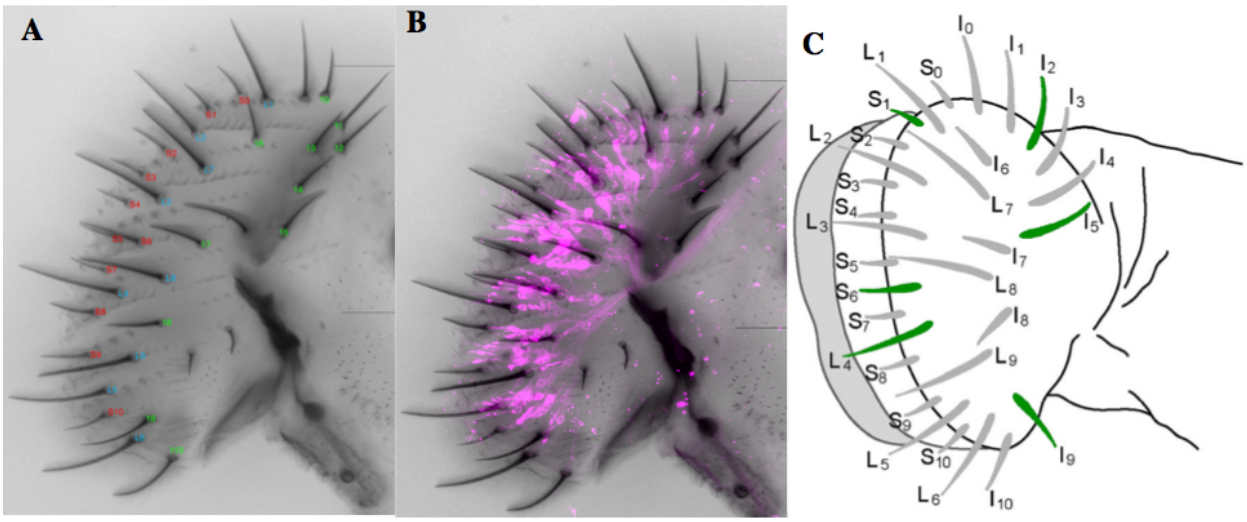
A
B
C
D
Gr64f
Gr66a
ppk28
ppk23
Sensilla:
S1
S6
L4
I2
I5
I9
GRN-LexA; LexAop-GFP
Ir76b-Gal4; UAS-cd8:tdtom
merge

Figure 3.4 Ir76b expression in the labellum
(A-C) Single labellar palp or (D) representative individual sensilla from flies expressing CD8::tdTomato (magenta) under the control of Ir76b-Gal4. (A) Labelled sensilla of a labellar palp with (B) Ir76b expression shown in each sensilla. (C) Cartoon of single labellum, green indicates specific sensilla, S1, S6, L4, I2, I5, and I9 used to show (D) overlap with different GRNs. All GRNs expressing GFP (green) under the control of Gr64f-LexA, Gr66a-LexA, ppk28-LexA, and ppk23-LexA respectively. White arrows indicate overlap observed between GRN population and Ir76b population. All images stained with antibodies and taken 25x.

3.4 Ir76b$^+$ cells overlap with many GRN populations

We also examined the expression pattern of Ir76b, since recent publications have implicated this receptor in the detection of a number of different ligands (Croset, 2016; Ganguly et al., 2017; Hussain et al., 2016; Zhang et al., 2013). We wanted to know if *Ir76b* in the labellum was co-labelled with other GRN populations, and if any overlapping expression of VGLUT$^+$ existed. We used *Ir76b-Gal4* to drive expression of cd8:tdtom and co-labelled with different GRNs using the lexA system to drive expression of GFP (Figure 3.4). We found that there are 2-3 Ir76b$^+$ cells in all S and L-type sensilla, one neuron in specific I-type, as well as expression in the taste pegs (Figure 3.5).

Ir76b$^+$ cells overlap with many GRN populations, as expected due to the many Ir76b$^+$ cells. There is co-expression between Ir76b$^+$ neurons and Gr66a$^+$ neurons in the S-type and I-b type sensilla (Figure 3.4 and 3.5). There is also co-labelling with all ppk28$^+$ neurons and Ir76b$^+$ neurons (Figure 3.4 and 3.5). There is overlap observed with gr64f$^+$ and Ir76b$^+$ cells in both S and L-type sensilla, as well as I-b type (Figure 3.4 and 3.5). This is expected as sugar sensing cells, specifically those found in I-type sensilla, have been reported as low-salt sensing neurons (Freeman and Dahanukar, 2015). Full co-labelling is observed between the ppk23$^+$ population and the Ir76b$^+$ population, indicating that some of the Ir76b$^+$ population does express VGLUT$^+$ (Figure 3.4 and 3.5). Importantly, given the diverse overlap with known GRN populations, *Ir76b-Gal4* does not appear to be a reliable marker of the low salt cell, as previously reported (Zhang et al., 2013).

Ir76b^{+} cells must also label other GRN populations that have not been accounted for. Specially, S4 and S8 have 2-3 Ir76b^{+} neurons where only one cell (a sugar neuron) has been accounted for (Figure 3.5). The I-type sensilla are the most unreliable and the least understood, although some Ir76b^{+} neurons show overlap with the sugar neurons, bitter neurons, and ppk23^{+} neurons in I-b type sensilla (Figure 3.5). This leaves some uncharacterized Ir76b^{+} cells throughout the labellum, and raises many questions about the biological relevance of Ir76b and what behaviors these neurons are responsible for.

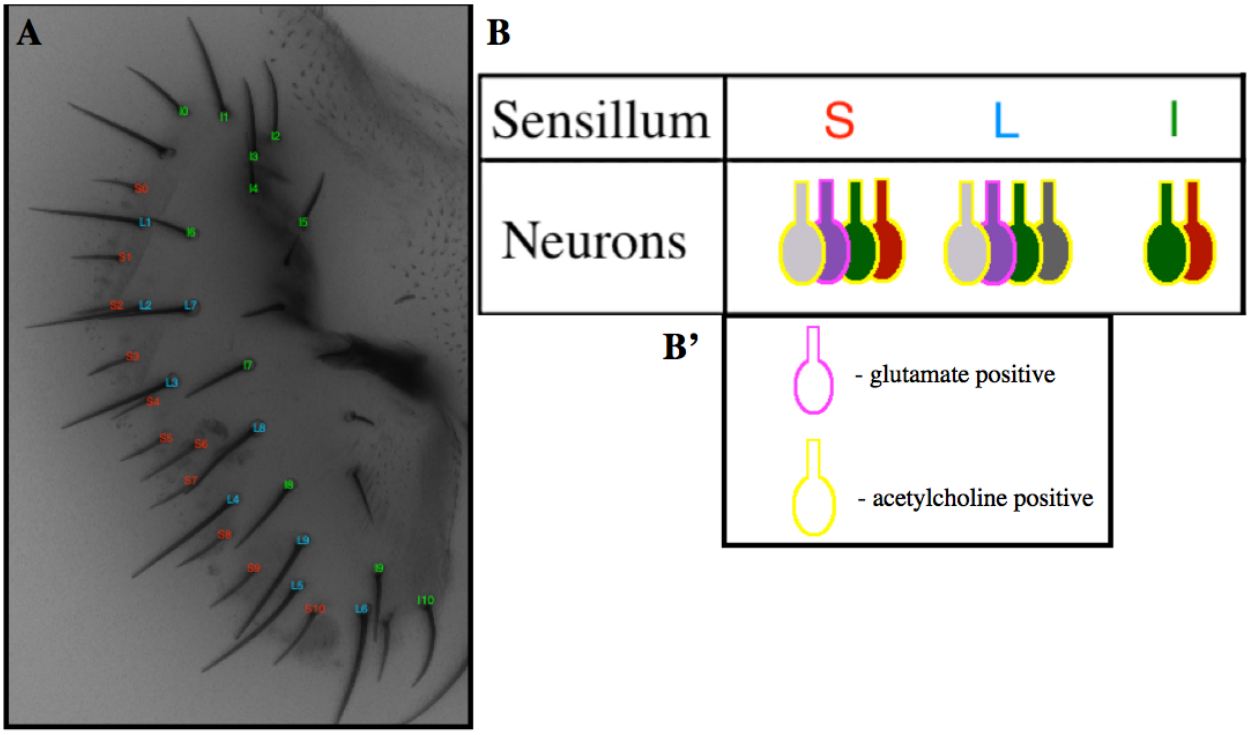

C

	S0	S1	S2	S3	S4	S5	S6	S7	S8	S9	S10	L1	L2	L3	L4	L5	L6	L7	L8	L9	I0	I1	I2	I3	I4	I5	I6	I7	I8	I9	I10
Gr66a	+	+	+	+		+	+	+		+	+										+	+	+	+	+	+	+	+	+	+	+
Gr64f	+	+	+	+	+	+	+	+	+	+	+	+	+	+	+	+	+	+	+	+	+	+	+	+	+	+	+	+	+	+	+
PPK23	+	++	++	+		+	++	++		++	++	+	+	+	+	+	+	+	+	+	+						+			+	
PPK28	+	+	+				+	+			+	+	+	+	+	+	+	+	+	+											
IR76b	+ ++	++ ++	++ ++	++ ++	++ +	++ ++	++ ++	++ ++	++ +	++ ++	++ ++	++ ++	++ ++	++ ++	++ ++	++ ++	++ ++	++ ++	++ ++	++ ++							++	+	++	++ ++	++
vGluT	+	+	+	+	+	+	+	+	+	+	+	+	+	+	+	+	+	+	+	+	+						+		+	+	
VAChT	++ +	++ +	++ +	++ +	++ +	++ +	++ +	++ +	++ +	++ +	++ +	++ +	++ +	++ +	++ +	++ +	++ +	++ +	++ +	++ +	++	++	++	++	++	++	++	++	++	++	++

Figure 3.5 Labellar staining summary
(A) Single labellar palp with labelled sensilla (B) corresponding to cartoon breakdown of different neurons housed in each sensilla type. Each neuron color indicates the receptors found to label the population with outline color (B') indicating the possible neurotransmitter each neuron uses to communicate. (C) Chart shows a + for every neuron

found in each sensilla (columns), color coded to match neuron population, receptor (top 5 rows), and NT type (bottom 2 rows). The square is empty if no neuron is present and a black + indicates an unknown cell.

3.5 Anatomy of neuronal populations in each sensillum of the labellum

Through all the labelling of different neuronal populations, we gained a clearer understanding of the organization of GRNs (Figure 3.5). Of particular interest is that, while most of the neurons are $ChAT^{+}$, a new population has been identified that is $VGLUT^{+}$ and expresses ppk23. This novel $VGLUT^{+}$ population, is present in the S-type, L-type, and specific I-type sensilla of the labellum. Another notable finding is that L-type sensilla house one sugar/Ir76b neuron, one $ppk23^{+}$/Ir76b neuron, and one water/Ir76b neuron (Figure 3.5). This leaves one uncharacterized neuron per sensillum, which is likely to be the 'low salt' neuron previously detected by electrophysiology (Figure 3.4; Hiroi et al., 2004).

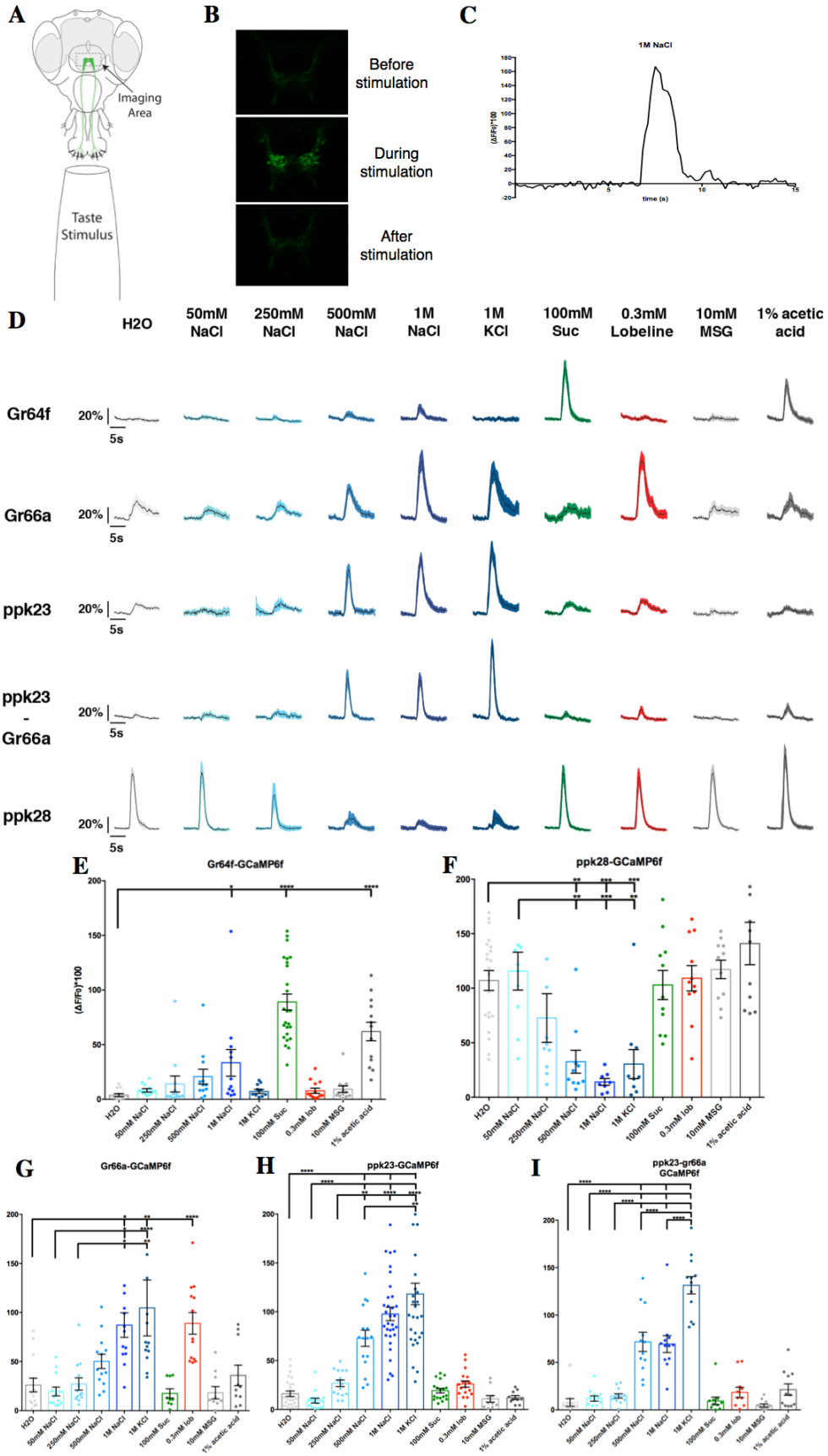
A
Imaging Area
Taste Stimulus
B
Before stimulation
During stimulation
After stimulation
C
1M NaCl
(ΔF/Fo)*100
time (s)
D
H2O
50mM NaCl
250mM NaCl
500mM NaCl
1M NaCl
1M KCl
100mM Suc
0.3mM Lob
10mM MSG
1% acetic acid
Gr64f
Gr66a
ppk23
ppk23 - Gr66a
ppk28
20%
5s
E
Gr64f-GCaMP6f
F
ppk28-GCaMP6f
G
Gr66a-GCaMP6f
H
ppk23-GCaMP6f
I
ppk23-gr66a GCaMP6f

Figure 3.6 Receptive fields of labellar sensory neurons
(A) Preparation for imaging of sensory neurons (adapted from LeDue EE et al., 2016) (B) example fluorescence change of ppk23-gal4 labellar projections before, during, and after a 1M NaCl stimulation, (C) example curve of this stimulation. (D-I) Change in the fluorescence of GCaMP6f driven under the control of different GRN-Gal4 populations. (D) Curve averages (n=9-20) of 10 different stimuli over 15 seconds. H20, 50mM NaCl, 250mM NaCl, 500 NaCl, 1M NaCl, 1M KCl, 100mM sucrose, 0.3mM lobeline, 10mM MSG, 1% acetic acid were stimulated on the labellum of the fly. (E-I) Scatter graph of maximum ΔF/F(%) for each GRN population. Error bars indicate standard error of the mean, one way ANOVA,*p<0.05, **p<0.01, ***p<0.001, ****p<0.0001.

3.6 Response palate of GRN populations

Much research has been done showing sensory neurons responses to specific stimuli over the years, but a comprehensive array of stimuli over many GRN populations still does not exist. Moreover, indications of salt responses between different GRNs have been shown but never looked at in detail. We used calcium imaging to monitor responses in labellar projections while stimulating the fly with a panel of tastants. We chose tastants to represent the most common modalities the fly responds to: bitter, sugar, acids, amino acid, water, and different salt concentrations. The strength of a response is reported as a percent of ΔF/F, which is the change in fluorescence from baseline after the stimuli is applied to the labellum.

3.6.1 ppk23^{+} labellar neurons respond strongly to increasing concentrations of salt

Although ppk23^{+} neurons have been shown to be responsive to a mixture of pheromones on the labellum, the responses are weak, suggesting that there may exist other ligands for these neurons (Thistle et al., 2012). Given that the anatomy of labellar ppk23^{+} cells did not mirror exactly what is found in the legs, we were interested in further defining the receptive fields of these neurons. *ppk23-Gal4* and *ppk23-lexA* have complete overlap in the GRN populations that they label (not shown).

We found that ppk23^{+} neurons on the labellum respond very strongly to increasing sodium salt concentrations (Figure 3.6). No significant response is seen from a stimulation with 50mM NaCl, which is considered to be an appetitive salt concentration. Larger responses are

observed from 1M NaCl, which is considered to be an aversive salt concentration (Figure 3.6). The responses appear to linearly increase with accumulating salt concentration. An even stronger response is seen from 1M KCl, indicating ppk23^{+} neuron tuning is not restricted to sodium salts.

Because ppk23^{+} neurons responded so strongly to salt, and there have been other salt-responsive populations previously reported, we wanted to examine salt responses across all the molecularly-identified populations of neurons. Gr66a^{+} neurons, which are known to respond to bitter compounds, respond strongly to increasing concentrations of salt, similar to ppk23^{+} neurons. These neurons are also not sodium specific, which is a hallmark of a high-salt response. Gr64f^{+} neurons, which are known to respond to sugar compounds, respond weakly to increasing concentrations of salt. These responses, unlike those in ppk23^{+} and Gr66a^{+} neurons, are sodium specific. ppk28^{+} neurons, known to responds to the osmolality of a substance, responds strongly to low salt concentrations and decreases in intensity as the compound's concentration increases.

Due to the neuron population staining that indicated overlap between ppk23^{+} and gr66a^{+} neurons in the S-type sensilla, as well as the similar pattern between the salt responses, we wanted to verify that the responses observed in the ppk23^{+} projections were not solely from the subset that co-expresses Gr66a. We took advantage of the gal80 system to restrict the Gal4 expression of ppk23 to any neurons not also expressing Gr66a-lexA. What we observed was very similar response patterns, with tighter curves and less variation (Figure 3.6). This ppk23^{+} population represents only the neurons that are VGLUT^{+} and shows strong responses to increasing concentrations of salt, very similar to *ppk23-Gal4*.

3.6.2 GRN populations primarily respond to expected tastants

Each labellar GRN population, with the exception of ppk23^{+}, has been previously characterized by their narrow receptive fields. Gr66a^{+} neurons showed an expected response to

the bitter compound, lobeline. ppk28^{+} also showed an expected response to most stimuli, previously described as a water response. Gr64f^{+} neurons showed an expected response to sugar, as well as an unexpected response to acetic acid (Figure 3.6).

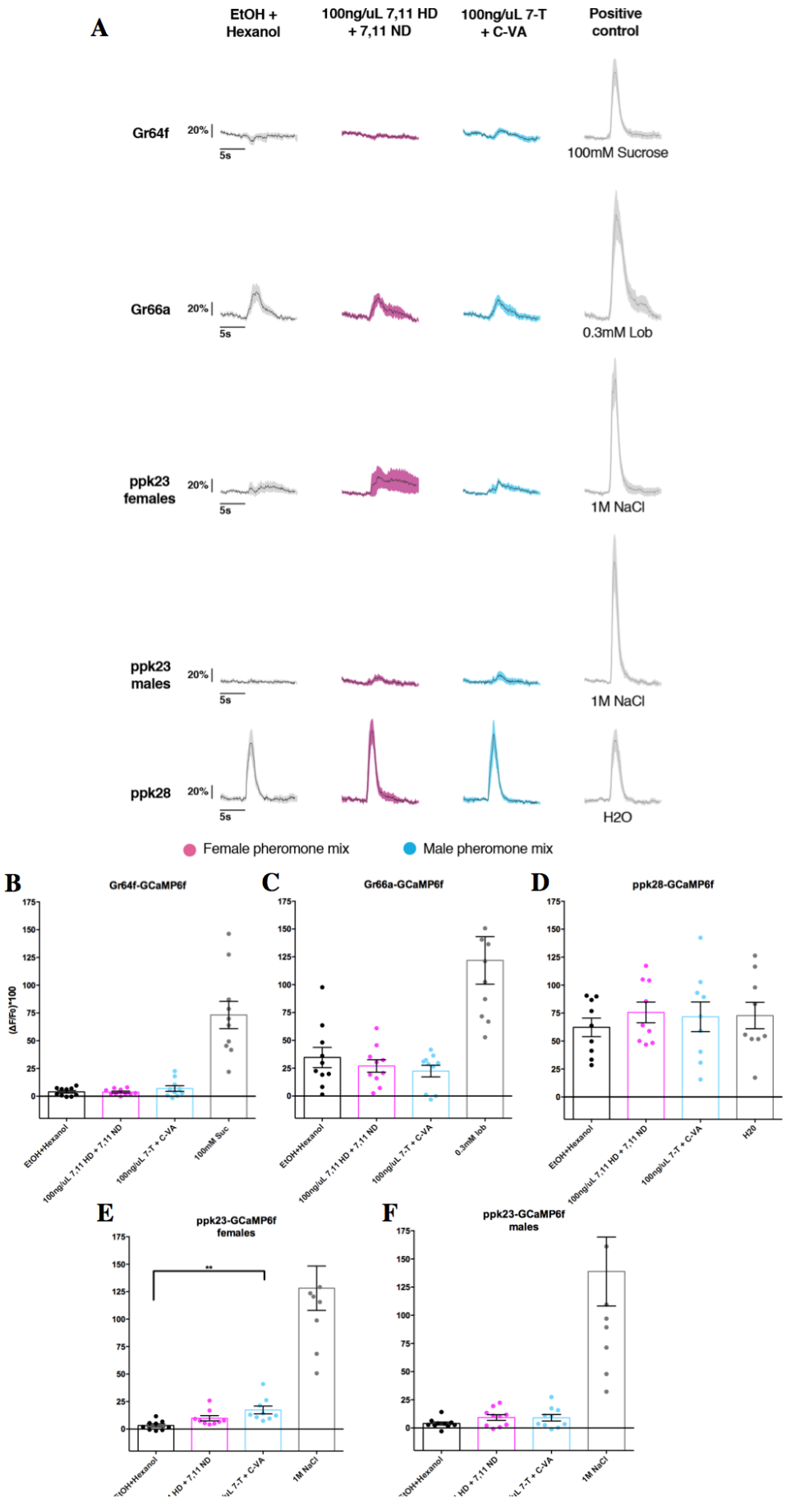
A
EtOH + Hexanol
100ng/uL 7,11 HD + 7,11 ND
100ng/uL 7-T + C-VA
Positive control
Gr64f
20%
5s
100mM Sucrose
Gr66a
0.3mM Lob
ppk23 females
1M NaCl
ppk23 males
ppk28
H2O
Female pheromone mix
Male pheromone mix
B
Gr64f-GCaMP6f
C
Gr66a-GCaMP6f
D
ppk28-GCaMP6f
(ΔF/F0)*100
EtOH+Hexanol
100ng/uL 7,11 HD + 7,11 ND
100ng/uL 7-T + C-VA
100mM Suc
0.3mM lob
H20
E
ppk23-GCaMP6f females
**
1M NaCl
F
ppk23-GCaMP6f males

Figure 3.7 Pheromone sensing in sensory neuron populations
(A-F) Change in the fluorescence of GCaMP6f driven under the control of different GRN-Gal4 populations. (A) Curve averages (n=9-12) of 4 different stimuli over 15 seconds stimulations. 2% EtOH+hexanol, female pheromone mix: 100ng/ul 7,11-heptacosadiene (7,11-HD) + 7,11-nonacosadiene (7,11-ND), male pheromone mix: pheromones 7-tricosene (7-T) + cis-vaccenyl acetate (c-VA), and an appropriate positive control were stimulated on the labellum of the fly. (B-F) Scatter graph of maximum ΔF/F(%) of (B) Gr64f-gal4, no response to pheromones. (C) Gr66a-gal4 responds weak to EtOH+hexanol. (D) ppk28-gal4 responds to osmolality. (E) female ppk23-gal4 responds weak to the male pheromone mix (F) male ppk23-gal4 does not respond to any pheromones in a significant way. Error bars show standard error of the mean, one way ANOVA, **p<0.01.

3.7 Female ppk23$^+$ labellar neurons respond weakly to male pheromones

Since ppk23$^+$ neurons on the legs have been previously reported as responding to pheromones, we wanted to test pheromone responses on the labellum in more detail. We used two pheromone mixtures, as described previously (Kallman et al., 2015). A "female" mixture of 7,11-HD and 7,11-ND and a "male" mixture of 7-T and c-VA were each presented at 100ng/ul diluted in 2% EtOH and Hexanol (Kallman et al., 2015). We used a 2% EtOH and hexanol solution as a vehicle control.

Similar to what was previously described, labellar responses to pheromones were low in amplitude. We observed no response from female flies to the alcohol control solution, as expected. A very small response is seen from the female pheromone mix that is not significantly different from the control (Figure 3.7). However, a small but significant response is seen from the male mix of pheromones (Figure 3.7). 1M NaCl was used as a positive control and elicits the expected high response.

3.7.1 Male ppk23$^+$ labellar neurons do not respond to pheromones

We next wondered whether there is a difference between male and female flies' response to the pheromone mixes. Because we know that ppk23$^+$ neuron anatomy in the labellum looks to be identical between the sexes, we wanted to see if that was true for their physiology. Like female ppk23$^+$ neurons, male ppk23$^+$ neurons showed small responses to both pheromone mixtures, although neither was significantly elevated compared to the vehicle control (Figure

3.6). Once again 1M NaCl was used as a positive control and showed a consistently high response.

3.7.2 No other labellar GRNs respond to pheromones

Since bitter neurons have been reported to respond to some male pheromones, we decided to look at pheromone responses across all the identified GRN types (Lacaille et al., 2007; Moon et al., 2009). $Gr64f^{+}$ sugar sensing neurons had no response to the vehicle, the male mix, or the female mix, yet still responded normally to the positive 100mM sucrose control (Figure 3.7). $ppk28^{+}$ water neurons responded to all solutions without significant difference, suggesting that this was just a water response. $Gr66a^{+}$ neurons showed responses to both pheromone mixtures, but also responded to the vehicle, which precluded any definitive conclusions. (Figure 3.7).

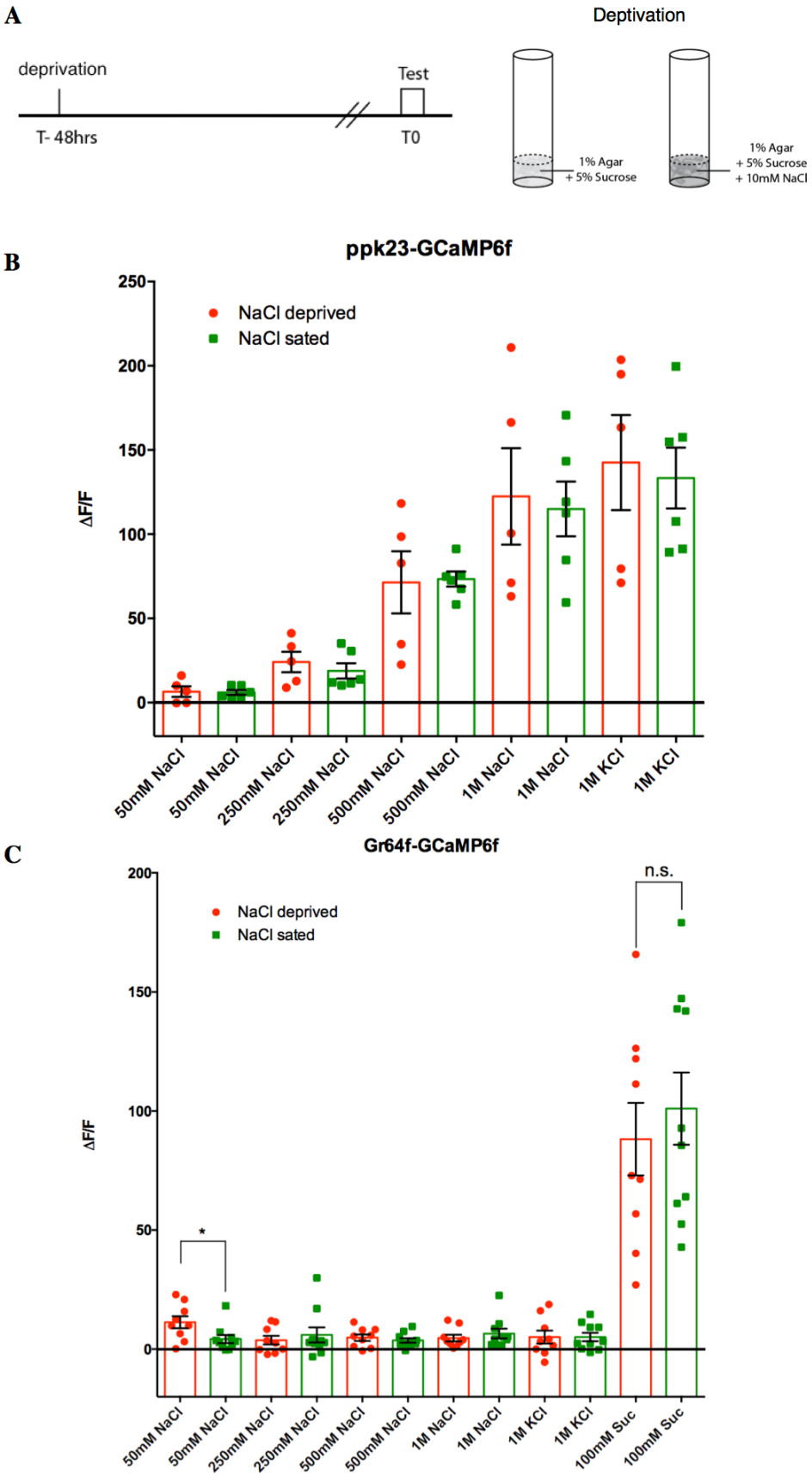
A
deprivation
Test
T- 48hrs
T0
Deptivation
1% Agar
+ 5% Sucrose
1% Agar
+ 5% Sucrose
+ 10mM NaCl
B
ppk23-GCaMP6f
NaCl deprived
NaCl sated
ΔF/F
250
200
150
100
50
0
50mM NaCl
50mM NaCl
250mM NaCl
250mM NaCl
500mM NaCl
500mM NaCl
1M NaCl
1M NaCl
1M KCl
1M KCl
C
Gr64f-GCaMP6f
NaCl deprived
NaCl sated
n.s.
*
ΔF/F
200
150
100
50
0
50mM NaCl
50mM NaCl
250mM NaCl
250mM NaCl
500mM NaCl
500mM NaCl
1M NaCl
1M NaCl
1M KCl
1M KCl
100mM Suc
100mM Suc

Figure 3.8 The effects of salt deprivation on GRN responses
(A) Flies deprived for 48 hours on 1% agar medium containing 5% sucrose (green) or 5% sucrose + 10mM NaCl (red). (B-C) Scatter graph of maximum ΔF/F(%) of GCaMP6f driven under the control (B) ppk23-gal4 shows an insignificant trend for increased response after salt deprivation to salt. (C) GCaMP6f driven by Gr64f-gal4 shows a significant increase in salt deprived flies to 50mM NaCl. Unpaired t-test, *p<0.05

3.8 Salt deprivation changes GRN sensitivity

We know that when flies are starved their sweet and bitter neurons sensitivity is increased and decreased, respectively (Inagaki et al., 2014). We therefore wondered whether salt deprivation had any effect on the sensory responses we observe to salt stimuli. To compare salt deprived versus undeprived responses, female flies were placed on a 1% agar medium containing 5% sucrose alone or 5% sucrose with 10mM NaCl for 48 hours (Figure 3.8A). We did not observe a significant change in ppk23^{+} GRN sensitivity following salt deprivation (Figure 3.8). On the other hand, Gr64f^{+} neurons showed an increase response to the lowest salt concentration, but no difference at higher concentrations (Figure 3.7). The flies were tested for their response to all salt concentrations previously tested, and if necessary a positive control. The flies were also stimulated with 100mM sucrose with no change in sensitivity to sugar observed (Figure 3.7).

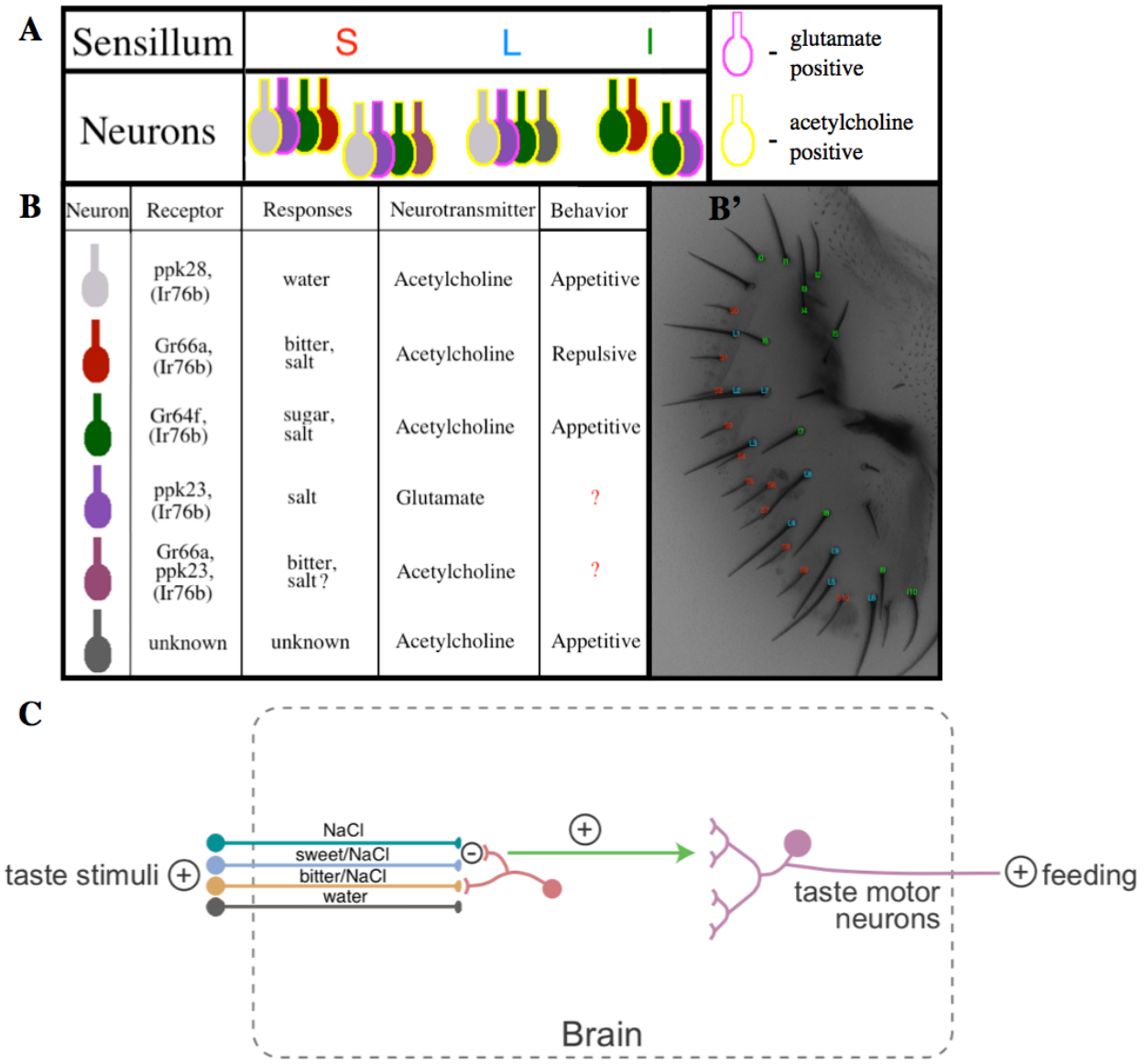

Figure 3.9 Salt is coded in a combinatorial way
(B') Single labellar palp with labelled sensilla (A) corresponding to cartoon breakdown of different neurons housed in each sensilla type. Each outline color indicates the possible neurotransmitter each neuron uses to communicate, (B) while the neurons color indicates the receptors found to label the population. A list of receptors, responses, NT, and behavior elicited by activation of neuronal population is summarized. (C) Diagram shows combinatorial mechanism in which sensory neurons all respond to salt, with possible GABAergic interneurons, to drive downstream feeding behavior.

4 Discussion

The evidence presented here has shown that: (1) ppk23^{+} neurons reside in the S and L-type sensilla of the fly labellum, organized in a combination of singlets and doublets; (2) The ppk23^{+} labellar population is VGLUT^{+}, with the exception of the six overlapping Gr66a^{+} neurons, which are ChAT^{+}; (3) ppk23^{+} labellar GRNs respond to increasing concentrations of salt independent from the overlapping Gr66a^{+} population; (4) All GRN populations tested show some response to salt. Thus, salt appears to be coded in a fashion similar to that seen in the olfactory system where a combination of activated neuron populations encodes stimulus identity. With a novel NT being attributed to the ppk23^{+} labellar population, additional questions about salt coding are raised. We have found where VGLUT^{+} neurons reside, and its high likelihood of contributing to salt coding; however, the true function of glutamate in the neural network is still unknown.

4.1 The labellar neuron map

4.1.1 Labellar GRN anatomy and physiology

Through staining and stimulating most of the large populations within the labellum, conclusions about what GRN population exists, where they reside, and what they respond to can be made. ppk28^{+} labellar neurons reside in select S-type sensilla and all L-type sensilla, are acetylcholine positive, and respond to water or low osmolality (Figure 3.6 and 3.9). Gr64f^{+} labellar neurons reside in all sensilla, are acetylcholine positive, and respond strongest to sugar, but also to acetic acid and weakly to NaCl (Figure 3.4, 3.5, and 3.8). Gr66a^{+} labellar neurons reside in most S-type sensilla and all I-type sensilla, are acetylcholine positive, and respond to bitter stimuli as well as high salt (Figure 3.4, 3.5, and 3.8). Ir76b is expressed in most identified GRNs (Figure 3.4 and 3.5).

ppk23^{+} labellar neurons reside in most S-type sensilla, all L-type sensilla, and few I-type sensilla, they are glutamate positive, and respond strongly to high salt as well as weakly to male pheromones (Figure 3.4, 3.5, 3.6 and 3.8). The Gr66a^{+}/ppk23^{+} labellar neurons exist in S1, S2, S6, S7, S9 and S10, which comprise almost all of the S-a type sensilla. They are positive for acetylcholine and appear to respond to high salt and bitter solutions, although were never tested in isolation (Figure 3.1, 3.4, and 3.5). To test the Gr66a^{+}/ppk23^{+} population in isolation, a similar method to that used in Figure 3.3 could be done, utilizing the FLPout system to restrict expression to the overlap between *Gr66a-lexA* and *ppk23-gal4*. This would allow isolation of this population for calcium imaging and behavioral assays.

To revisit the original findings from Makoto Hiroi where he classifies each S and L-type sensillum to contain the four cells W, S, L1, and L2, we can reclassify these cells using our findings (2002). The W cell, responding to water, is an osmolality sensor that can be found in all L-type and half of the S-type sensilla and is co-expressed with Ir76b^{+} (Figure 5). The S cell is cholinergic, responds to sugar, acetic acid, and sodium salt, can be found in all sensilla and expresses Ir76b^{+} in all but one case (Figure 5). The L2 cell (L2a) is cholinergic, responding to bitters and high salt, can be found in most S-type and all I-type sensilla and expresses Ir76b^{+} in select cells (Figure 5). A second L2 cell (L2b) is glutamatergic, has been identified that responds only to high salt, can be found in most S-type, all L-type, and a few I-type sensilla, and co-expressed Ir76b^{+} in all but one of these cells (Figure 5). Finally a the third L2 cell (L2c), is cholinergic and is found in S1, S2, S6, S7, S9, and S10, is unknown in its response pattern but is expected to respond to both bitter and high salt compounds and expresses Ir76b (Figure 5). This L2c cell is considered to be different than the L2a cell as it expresses ppk23. At this point the L1 cell remains unknown. It appears to be in part the same as the S cell, but is likely a separate

population still unidentified in the L-type sensilla. Using the two binary expression systems to subtract all known GRNs (Gr64f, Gr66a, ppk28, ppk23) from a pan-GRN driver would in theory isolate this population that could then be employed with calcium imaging to confirm its response pattern.

4.1.2 Ir76b$^+$ neurons in the labellum

The Ir76b-gal4 population appeared more promiscuous in the labellum than previously thought. Because it overlaps with all of the populations of neurons tested in immunolabelling experiments, it became less interesting to look at the receptive field of these neurons. By looking at the receptive fields of all the GRNs tested, and knowing what we do about the overlap with these and *Ir76b-gal4*, we can assume that it would respond to all stimuli. It is unknown whether if all the neurons that are found in Ir76b-gal4 are actually Ir76b$^+$, or if they are salt responsive. It has been shown that the *Ir76b* may be a widely-expressed receptor that may pair with other ionotropic receptors to produce functional channels (Ganguly et al., 2017). In this case, *Ir76b* may work in different complexes in different cell types, leading to different responses to ligands. It would be interesting to use *Ir76b* mutants in conjunction with the different GRN-Gal4s in an attempt to rescue a salt response, indicating the population of cell sufficient to elicit a salt response.

Understanding which neuron populations express the Ir76b receptor, if separate from what is seen in *Ir76b-Gal4*, could give insight as to if the receptor works in a complex, what other receptors are necessary, and which neuron population is responsible for the low salt taste. It has been suggested that low salt taste is restricted to Ir76b$^+$ cells found in the L-type sensilla, and Ir76b$^+$ cells in taste pegs are required for amino acid taste (Zhang et al., 2013; Ganguly et al., 2017). From our staining we know that it is unlikely that the Ir76b$^+$ cells responsible for sensing

low salt are restricted to the L-type sensilla, as the receptor appears to be in many cells across many sensilla types. It would be interesting see if the loss of low salt attraction that is observed in *Ir76b* mutants could be rescued with one of the GRN populations (Zhang et al., 2013). Additionally, we know that *Ir76b* is sufficient to elicit a salt response, and Δppk23 mutant flies show no significant deficit in the normal detection of salt with PER behavior, therefore it is possible that Ir76b is the necessary receptor within the ppk23^{+} population to evoke a salt response (Zhang et al., 2013; Thistle et al., 2012).

4.2 ppk23^{+} labellar neurons as salt sensors

4.2.1 VGLUT^{+} cells are glutamatergic

It is likely that the ppk23^{+} population, excluding the neurons that overlap with *Gr66a*, is glutamatergic. These cells are positive for *VGLUT-Gal4*, which makes it probable that they express VGLUT, although formally, this could be an artifact of the Gal4 expression construct. However, two lines of evidence suggest that this is not the case: first, both the *DVGLUT-Gal4* promoter-Gal4 fusion (not shown) and the *VGLUT-Gal4* Trojan transgene coupled with native gene (line used for labeling) show overlap with *ppk23-Gal4*; second, these are the only GRNs that are not ChAT-Gal4^{+}, suggesting that acetylcholine is not present in these cells.

It is also important to recognize the VGLUT expression alone does not necessarily mean that the neurons release glutamate. Although VGLUT is necessary for the packaging and release of glutamate, it is not sufficient for glutamate to be present. It does, however, make it highly likely. Moreover, the fact that these neurons appear to not express ChAT also supports the idea that they are very likely to be glutamatergic. However, it is formally possible at this point that another neurotransmitter, such as octopamine, is released by these GRNs.

4.2.2 ppk23$^+$/Gr66a$^+$ neurons are an isolated population that remains uncharacterized

The six ppk23$^+$ cells that are not VGLUT$^+$ are instead positive for ChAT$^+$, as well as overlap with the Gr66a$^+$ population. This indicates a sub-population for both *ppk23* and *Gr66a* in the labellum. This finding is interesting because ppk23$^+$ cells in the legs are shown to be consistently present in doublets, appearing to be responsible for pheromone sensing and required in mating (Kallman et al., 2015). It is therefore unsurprising that there are doublets in the ppk23$^+$ population that exist on the labellum, with one being VGLUT$^+$ and the other ChAT$^+$; however, it is surprising that the anatomy is inconsistent throughout the entire population. Interestingly, the ppk23$^+$/ChAT$^+$ neurons that overlap with the Gr66a$^+$ population have not been reported in the legs. When looking at the receptive fields of these two neuron populations, it is less surprising that there is a shared population as they both respond similarly to high salt. Because of the gal80 experiment we know that the ppk23$^+$- Gr66a$^+$ population is still salt responsive, indicating that the bitter receptor is not necessary for the salt response (Figure 3.5). It is possible that the Gr66a$^+$ projection response to salt requires the *ppk23* channel, however it is unlikely due to previous experiments showing high salt responses from I-type sensilla that do not contain ppk23$^+$ cells (Hiroi et al., 2002). A way to address this would be to use gal80 to restrict *Gr66a-Gal4* to those neurons that do not express *ppk23-lexA*, and using calcium imaging to examine whether these cells also show a salt response.

It is important to look at each of these populations independently and with respect to glutamate function. ppk23$^+$, gr66a$^+$, gr66a$^+$ - ppk23$^+$, ppk23$^+$ - gr66a$^+$, ppk23$^+$ + gr66a$^+$, and ppk23$^+$/gr66a$^+$ can all be used in silencing and activation experiments to characterize the behavioral roles of these different populations. We already know what the calcium imaging response pattern is from ppk23$^+$, gr66a$^+$, and ppk23$^+$ - gr66a$^+$, but all other populations' receptive

field would also be useful. Once a better understanding of the valence of these neuron populations toward salt is understood, glutamate RNAi can be used to see if these effects are dependent on glutamate transmission. This would help better confirm that this NT is responsible for signaling downstream.

4.2.3 ppk23^{+} neurons are not F or M cells

The anatomy of ppk23^{+} cells resembles that seen in the legs with the six sensilla that contain doublets. Therefore, we wondered whether the labellum had the same F and M cells reported in the legs. The ppk23^{+} population showed a weak response to pheromones found on the male cuticle, similar to that seen from the M-cell on the legs (Kallman et al., 2015). If the other neuron in the doublet is then the F-cell, and specific to the female pheromones, we would see a response in the Gr66a^{+} population as it overlaps with the VGLUT^{-}, or ChAT^{+}, population. However, no response to female pheromones was observed in the Gr66a^{+} population.

One caveat, is that because the ppk23^{+} population still includes the ChAT^{+} cells, these could be muting the responses between the different pheromones. Also, the Gr66a^{+} cells that do not contain *ppk23* could be contributing to the responses observed, masking the true receptive field of these six neurons. Gr66a^{+} cells also show a response to EtOH, which might be masking any pheromone responses. The best way to answer these questions would be to restrict the two neuron populations with the previous genetic constructs mentioned and stimulate them with the isolated male and female pheromones. An additional caveat is that the hydrocarbons are not water soluble. These tastants were dissolved in EtOH and Hexanol, but were then diluted out to a 2% alcohol concentration in H20 to minimize the possible aversive qualities of these solvents. It could be that these sensilla were not actually being stimulated consistently with the concentration of the pheromones that was intended. Much mixing was done before each labellar stimulation in

an attempt to mitigate this problem, but could not be properly controlled for. It may be possible to stimulate the flies' proboscis with the live cuticle of a male or virgin female fly, which would contain the proper hydrocarbons and tease out the issues with dilutions and solubility (Clowney et al., 2015). This would not, however, control for all the other compounds found on the cuticle or identify which compounds and what concentrations elicit a response, if a response is observed.

It might be true that the ppk23^{+} labellar populations are involved in more than salt taste. We know that the ppk23^{+} labellar population responds to salt, we know the ppk23^{+} tarsal population is involved in courtship, and we know that after mating salt becomes more appetitive (Kallman et al., 2015; Walker et al., 2015). It is possible that salt taste is involved in courtship and ppk23^{+} neurons play a role in this. It would be interesting to look at salt preference after mating when the ppk23^{+} population is silenced. This could be done at different temporal points using optogenetics and with different degrees of salt deprivation. It also might be interesting to see if females have a preference in the composition of the medium in which they lay their eggs, with respect to salt concentration. Is this affected when the ppk23^{+} population is activated or silenced? Can ppk23^{+} cells be used to rescue any behavioral phenotypes observed with Ir76b^{+} population silencing?

4.2.4 Glutamatergic cells play a role in salt sensing

Exactly how glutamate is working and what it is doing in these cells is still unknown. Characterizing glutamate's role in ppk23^{+} cells and the neural circuit is the next step in understanding salt taste. To characterize glutamate in these cells, glutamate RNAi could be driven in ppk23^{+} cells to alter salt behavior. Once the valence of ppk23^{+} cells is known, RNAi for glutamate could be used to phenocopy that seen when ppk23^{+} cells are silenced. Additionally, using GFP recombination across synaptic partners (GRASP) to find cells downstream of these

VGLUT$^+$/ppk23$^+$ cells would further help to understand the circuit. Again glutamate RNAi could be used in the sensory neurons to show that a loss of activity is achieved in identified downstream neurons through the use of GCaMP driven in neurons synaptically connected in this circuit.

4.3 Gr66a$^+$ labellar neurons as salt sensors

My observation that Gr66a$^+$ neurons respond to high salt is consistent with past reports (Marella et al., 2006). It would be interesting to test the behavioral effect of Gr66a GRN silencing on high salt avoidance, by using a die based binary choice assay (LeDue et al., 2016). Additionally, it would be interesting to look at the difference between S-a and S-b sensilla neuron populations' receptive field with respect to salt (Freeman and Dahanukar, 2015). Using bitter receptors isolated to these sensilla subgroups, Gr36b-Gal4 expressed in S-a and Gr22f-Gal4 expressed in S-b, could be used with GCaMP to observed a possible difference in salt response. This would help to inform the questions about the bitter neuron population that overlaps with ppk23$^+$ population, and whether there is a difference in their salt sensitivity.

4.4 Salt taste coded combinatorially

ppk23$^+$ cells, Gr66a$^+$ cells, Gr64f$^+$ cells, and ppk28$^+$ cells all responded to salt in some way (Figure 3.6 and 3.9). Whether strong or weak excitation, or inhibition by solute concentration, all these GRNs presumably contribute to the fly's understanding of salt within a given solution. The different sensory neuron populations each have unique receptive fields, that project downstream to either promote or reject feeding behavior. Each of these sensory neurons found on the labellum can be classified by what elicits the largest response, and can all be quantified by their responsiveness to salt. Because all GRNs tested respond to salt, it has been revealed that salt is coded in a manner where the combination of activated GRNs must drive

feeding behavior (Figure 3.9). Although the way in which this circuit is constructed and works to contribute to feeding motivation is unknown, much is known about sensory coding in the sugar and bitter pathway that can help inform the salt pathway. It is possible that just like the feedback interaction between bitter and sugar neurons, there is a similar interaction between different salt sensing populations (Figure 3.9). We know that GABAergic interneurons play a role in feedback between these reciprocal pathways, and can therefore foresee a narrative where similar networking is in place for the salt pathway (Chu et al., 2014). This could possibly drive the switch between appetitive and aversive salt concentrations.

Salt taste has been overlooked for some time and has revealed some inconsistencies with the way we think about taste coding in flies. It appears to affect the firing of every neuron population in the fly labellum, indicating a combinatorial coding system. Salt is one of the only known tastant that switches between appetitive and aversive valence based on concentration, likely reflecting the importance of keeping salt consumption tightly controlled. Salt appears to play an important role in producing healthy offspring and has been correlated with increased aggression and decreased spatial memory in mammals (Walker et al., 2015; Naha et al., 2016; Liu et al., 2014). Understanding how high salt is processed in the brain and how that shapes behavior, both during and post-ingestion, are the next details that need to be addressed to interpret taste coding.

5 Conclusion

This study was set out to understand the way salt is processed across different sensory neurons in the labellum, and to find a role for glutamate in the labellum of the fly. A comprehensive array of response patterns of different salt concentrations and tastants representing different modalities across most segregated GRN populations was constructed. A novel labellar gustatory population, ppk23^{+} cells, were found to be glutamatergic and responsive to sodium and potassium salt. Although much about this ppk23^{+}/VGLUT^{+} population and salt taste processing is still unknown, this work reports that the paradigm previously set about the labeled lines coding in the gustatory system needs to be revisited. ppk23^{+}, Gr66a^{+}, Ir76b^{+}, Gr64f^{+} populations and subpopulations provide the first indication of combinatorial coding in the taste system with respect to salt. This work looks at how animals deal with contrasting cues from the same compound, integrating these different inputs to make decisions about what to ingest.

It is unknown whether these findings are applicable to high order animal taste systems. It would be unsurprising if the coding systems are conserved between organisms, as the feeding behavior toward salt appears to be consistent. What this means for humans is unclear; however, understanding how salt is coded, what effects it has on our behavior, and how that can be manipulated, all play into the understanding of diet. High salt containing meals are not unfamiliar to human societies, and what that means for our physical and mental health is often debated. Understanding the more simplistic gustatory system of the fruit fly can give insight to understanding our own systems, supplying a better understanding of how different eating habits contribute to health and lifespan. Salt is on every table, in every restaurant and every home, yet its effect on our brain and the important balance of ingestion remains unknown.

References

Alves, G., Sallé, J., Chaudy, S., Dupas, S., & Manière, G. (2014). High-NaCl perception in Drosophila melanogaster. *The Journal of Neuroscience : The Official Journal of the Society for Neuroscience*, *34*(33), 10884–91.

Andrés, M., Turiégano, E., Göpfert, M. C., Canal, I., & Torroja, L. (2014). The extracellular matrix protein artichoke is required for integrity of ciliated mechanosensory and chemosensory organs in Drosophila embryos. *Genetics*, *196*(4), 1091–1102.

Berck, M. E., Khandelwal, A., Claus, L., Hernandez-Nunez, L., Si, G., Tabone, C. J., … Cardona, A. (2016). The wiring diagram of a glomerular olfactory system. *eLife*, *5*(e14859)

Berridge, M. J. (1998). Neuronal calcium signaling. *Neuron*, *21*(1), 13–26.

Billeter, J.C., Atallah, J., Krupp, J. J., Millar, J. G., & Levine, J. D. (2009). Specialized cells tag sexual and species identity in Drosophila melanogaster. *Nature*, *461*(7266), 987–991.

Brand, A. H., & Perrimon, N. (1993). Targeted gene expression as a means of altering cell fates and generating dominant phenotypes. *Development*, *118*, 401–15.

Cameron, P., Hiroi, M., Ngai, J., & Scott, K. (2010). The molecular basis for water taste in Drosophila. *Nature*, *465*(7294), 91–95.

Chandrashekar, J., Kuhn, C., Oka, Y., Yarmolinsky, D. a, Hummler, E., Ryba, N. J. P., & Zuker, C. S. (2010). The cells and peripheral representation of sodium taste in mice. *Nature*, *464*(7286), 297–301.

Chen, T.-W., Wardill, T. J., Sun, Y., Pulver, S. R., Renninger, S. L., Baohan, A., … Kim, D. S. (2013). Ultrasensitive fluorescent proteins for imaging neuronal activity. *Nature*, *499*(7458), 295–300.

Chu, B., Chui, V., Mann, K., & Gordon, M. D. (2014). Presynaptic gain control drives sweet and bitter taste integration in Drosophila. *Current Biology*, *24*(17), 1978–1984.

Clarke, S. N. D. A., & Bernstein, I. L. (2001). NaCl preference increases during pregnancy and lactation: Assessment using brief access tests. *Pharmacology Biochemistry and Behavior*, *68*(3), 555–563.

Clowney, E. J., Iguchi, S., Bussell, J. J., Scheer, E., & Ruta, V. (2015). Multimodal Chemosensory Circuits Controlling Male Courtship in Drosophila. *Neuron*, *87*(5), 1036–1049.

Couto, A., Alenius, M., & Dickson, B. J. (2005). Molecular, anatomical, and functional organization of the Drosophila olfactory system. *Current Biology*, *15*(17), 1535–1547.

Croset, V., Rytz, R., Cummins, S. F., Budd, A., Brawand, D., Kaessmann, H., … Benton, R. (2010). Ancient protostome origin of chemosensory ionotropic glutamate receptors and the evolution of insect taste and olfaction. *PLoS Genetics*, *6*(8).

Croset, V., Schleyer, M., Arguello, J. R., Gerber, B., & Benton, R. (2016). A molecular and neuronal basis for amino acid sensing in the Drosophila larva. *Scientific Reports*, *6*, 34871.

Dahanukar, A., Foster, K., van der Goes van Naters, W. M., & Carlson, J. R. (2001). A Gr receptor is required for response to the sugar trehalose in taste neurons of Drosophila. *Nature Neuroscience*, *4*(12), 1182–6.

Dahanukar, A., Lei, Y. T., Kwon, J. Y., & Carlson, J. R. (2007). Two Gr Genes Underlie Sugar Reception in Drosophila. *Neuron*, *56*(3), 503–516.

Daniels, R. W., Gelfand, M. V., Collins, C. A., & DiAntonio, A. (2008). Visualizing glutamatergic cell bodies and synapses in Drosophila larval and adult CNS. *Journal of Comparative Neurology*, *508*(1), 131–152.

de Araujo, I. E., Geha, P., & Small, D. M. (2012). Orosensory and Homeostatic Functions of the Insular Taste Cortex. *Chemosensory Perception*, *5*(1), 6407.

del Valle Rodríguez, A., Didiano, D., & Desplan, C. (2012). Power tools for gene expression and clonal analysis in Drosophila. *Nature Methods*, *9*(1), 47–55.

Faas, M. M., Melgert, B. N., & De Vos, P. (2010). A brief review on how pregnancy and sex hormones interfere with taste and food intake. *Chemosensory Perception*, *3*(1), 51–56.

Ferveur, J. F. (2005). Cuticular hydrocarbons: Their evolution and roles in *Drosophila* pheromonal communication. *Behavior Genetics*, *35*(3), 279–295.

Fischler, W., Kong, P., Marella, S., & Scott, K. (2007). The detection of carbonation by the *Drosophila* gustatory system. *Nature*, *448*(06101), 1054–1057.

Freeman, E. G., & Dahanukar, A. (2015). Molecular neurobiology of Drosophila taste. *Current Opinion in Neurobiology*, *34*, 140–148.

Fujii, S., Yavuz, A., Slone, J., Jagge, C., Song, X., & Amrein, H. (2015). Drosophila sugar receptors in sweet taste perception, olfaction, and internal nutrient sensing. *Current Biology*, *25*(5), 621–627.

Fujishiro, N., Kijima, H., & Morita, H. (1984). Impulse frequency and action potential amplitude in labellar chemosensory neurones of Drosophila melanogaster. *Journal of Insect Physiology*, *30*(4), 317–325.

Ganguly, A., Pang, L., Duong, V., Lee, A., Schoniger, H., Varady, E., & Dahanukar, A. (2017). A Molecular and Cellular Context-Dependent Role for Ir76b in Detection of Amino Acid

Taste Article A Molecular and Cellular Context-Dependent Role for Ir76b in Detection of Amino Acid Taste. *CellReports*, *18*(3), 737–750.

Gendre, N., Lüer, K., Friche, S., Grillenzoni, N., Ramaekers, A., Technau, G. M., & Stocker, R. F. (2004). Integration of complex larval chemosensory organs into the adult nervous system of Drosophila. *Development*, *131*(1), 83–92.

Goodwin, S. F., Taylor, B. J., Villella, A., Foss, M., Ryner, L. C., Baker, B. S., & Hall, J. C. (2000). Aberrant Splicing and Altered Spatial Expression Patterns in fruitless Mutants of Drosophila melanogaster Stephen, *154*, 725–745.

Gordon, M. D., & Scott, K. (2009). Motor Control in a Drosophila Taste Circuit. *Neuron*, *61*(3), 373–384.

Hall, J. C. (1994). The mating of a fly. *Science*, *264*(5166), 1702–1714.

Hanukoglu, I., & Hanukoglu, A. (2016). Epithelial sodium channel (ENaC) family: Phylogeny, structure-function, tissue distribution, and associated inherited diseases. *Gene*, *579*(2), 95–132.

Harris, D. T., Kallman, B. R., Mullaney, B. C., & Scott, K. (2015). Representations of Taste Modality in the Drosophila Brain. *Neuron*, *86*(6), 1449–1460.

Hendel, T., Mank, M., Schnell, B., Griesbeck, O., Borst, A., & Reiff, D. F. (2008). Fluorescence changes of genetic calcium indicators and OGB-1 correlated with neural activity and calcium in vivo and in vitro. *The Journal of Neuroscience*, *28*(29), 7399–7411.

Hiroi, M., Marion-Poll, F., & Tanimura, T. (2002). Differentiated response to sugars among labellar chemosensilla in Drosophila. *Zoological Science*, *19*(9), 1009–1018.

Hiroi, M., Meunier, N., Marion-Poll, F., & Tanimura, T. (2004). Two antagonistic gustatory receptor neurons responding to sweet-salty and bitter taste in Drosophila. *Journal of Neurobiology*, *61*(3), 333–342.

Hussain, A., Zhang, M., Ucpunar, H. K., Svensson, T., Quillery, E., Gompel, N., … Grunwald Kadow, I. C. (2016). Ionotropic Chemosensory Receptors Mediate the Taste and Smell of Polyamines. *PLoS Biology*, *14*(5), 1–30.

Inagaki, H. K., Panse, K. M., & Anderson, D. J. (2014). Independent, reciprocal neuromodulatory control of sweet and bitter taste sensitivity during starvation in Drosophila. *Neuron*, *84*(4), 806–820.

Inoshita, T., & Tanimura, T. (2006). Cellular identification of water gustatory receptor neurons and their central projection pattern in Drosophila. *Proceedings of the National Academy of Sciences of the United States of America*, *103*(4), 1094–1099.

Jeong, Y. T., Oh, S. M., Shim, J., Seo, J. T., Kwon, J. Y., & Moon, S. J. (2016). Mechanosensory neurons control sweet sensing in Drosophila. *Nature Communications*, *7*(12872).

Jones, W. D., Cayirlioglu, P., Grunwald Kadow, I., & Vosshall, L. B. (2007). Two chemosensory receptors together mediate carbon dioxide detection in Drosophila. *Nature*, *445*(7123), 86–90.

Joseph R.M. and Carlson J.R. (2015). Drosophila chemoreceptors: A molecular interface between the chemical world and the brain. *Trends in Genetics*, *31*(12), 683–695.

Jourjine, N., Mullaney, B. C., Mann, K., & Scott, K. (2016). Coupled Sensing of Hunger and Thirst Signals Balances Sugar and Water Consumption. *Cell*, *166*(4), 855–866.

Kain, P., & Dahanukar, A. (2015). Secondary Taste Neurons that Convey Sweet Taste and Starvation in the Drosophila Brain. *Neuron*, *85*(4), 819–832.

Kallman, B. R., Kim, H., & Scott, K. (2015). Excitation and inhibition onto central courtship neurons biases drosophila mate choice. *eLife*, *4*(e11188), 1–18.

Kawano, T., Ryuda, M., Matsumoto, H., Ochiai, M., Oda, Y., Tanimura, T., … Hayakawa, Y. (2015). Function of desiccate in gustatory sensilla of drosophila melanogaster. *Scientific Reports*, *5*(17195).

Kundu, S., Ganguly, A., Chakraborty, T. S., Kumar, A., & Siddiqi, O. (2016). Synergism and Combinatorial Coding for Binary Odor Mixture Perception in Drosophila. *eNeuro*, *3*(4), 1–14.

Kwon, J. Y., Dahanukar, A., Weiss, L. A., & Carlson, J. R. (2007). The molecular basis of CO2 reception in Drosophila. *Proceedings of the National Academy of Sciences of the United States of America*, *104*(9), 3574–8.

Lacaille, F., Hiroi, M., Twele, R., Inoshita, T., Umemoto, D., Manière, G., … Ferveur, J. F. (2007). An inhibitory sex pheromone tastes bitter for Drosophila males. *PLoS ONE*, *2*(8), 1–7.

Lai, S.L., & Lee, T. (2006). Genetic mosaic with dual binary transcriptional systems in Drosophila. *Nature Neuroscience*, *9*(5), 703–709.

Ledue, E. E., Chen, Y., Jung, A. Y., Dahanukar, A., & Gordon, M. D. (2015). Pharyngeal sense organs drive robust sugar consumption in Drosophila. *Nature Communications*, *6*(6667).

LeDue, E. E., Mann, K., Koch, E., Chu, B., Dakin, R., & Gordon, M. D. (2016). Starvation-Induced Depotentiation of Bitter Taste in Drosophila. *Current Biology*, *26*(21), 2854–2861.

Ledue, E. E. (2016). *EXAMINING HOW PHARYNGEAL TASTE INPUT AND INTERNAL PHYSIOLOGICAL CONTEXT INFLUENCE FEEDING DECISIONS IN*.

Lemon, C. H., & Katz, D. B. (2007). The neural processing of taste. *BMC Neuroscience*, *8 Suppl 3*(S5).

Liu, L., Leonard, A. S., Motto, D. G., Feller, M. A., Price, M. P., Johnson, W. A., & Welsh, M. J. (2003b). Contribution of Drosophila DEG/ENaC genes to salt taste. *Neuron*, *39*(1), 133–146.

Liu, W. W., & Wilson, R. I. (2013). Glutamate is an inhibitory neurotransmitter in the Drosophila olfactory system. *Proceedings of the National Academy of Sciences of the United States of America*, *110*(25), 10294–9.

Liu, Y. Z., Chen, J. K., Li, Z. P., Zhao, T., Ni, M., Li, D. J., … Shen, F. M. (2014). High-salt diet enhances hippocampal oxidative stress and cognitive impairment in mice. *Neurobiology of Learning and Memory*, *114*, 10–15.

Lu, B., LaMora, A., Sun, Y., Welsh, M. J., & Ben-Shahar, Y. (2012). Ppk23-dependent chemosensory functions contribute to courtship behavior in drosophila melanogaster. *PLoS Genetics*, *8*(3).

Mahr, A., & Aberle, H. (2006). The expression pattern of the Drosophila vesicular glutamate transporter: A marker protein for motoneurons and glutamatergic centers in the brain. *Gene Expression Patterns*, *6*(3), 299–309.

Marella, S., Fischler, W., Kong, P., Asgarian, S., Rueckert, E., & Scott, K. (2006). Imaging taste responses in the fly brain reveals a functional map of taste category and behavior. *Neuron*, *49*(2), 285–295.

Masek, P., & Keene, A. C. (2013). Drosophila Fatty Acid Taste Signals through the PLC Pathway in Sugar-Sensing Neurons. *PLoS Genetics*, *9*(9).

McKellar, C. E. (2016). Motor control of fly feeding. *Journal of Neurogenetics*, *30*(2), 101–11.

Miyazaki, T., Lin, T.-Y., Ito, K., Lee, C.-H., & Stopfer, M. (2015). A gustatory second-order neuron that connects sucrose-sensitive primary neurons and a distinct region of the gnathal ganglion in the Drosophila brain. *Journal of Neurogenetics*, *29*(2–3), 144–155.

Moon, S. J., Lee, Y., Jiao, Y., & Montell, C. (2009). A Drosophila Gustatory Receptor Essential for Aversive Taste and Inhibiting Male-to-Male Courtship. *Current Biology*, *19*(19), 1623–1627.

Naha, D., Jhala, Y. V., Qureshi, Q., Roy, M., Sankar, K., & Gopal, R. (2016). Ranging, activity and habitat use by tigers in the mangrove forests of the Sundarban. *PLoS ONE*, *11*(4), 1–16.

Nakai, J., Ohkura, M., & Imoto, K. (2001). A high signal-to-noise Ca(2+) probe composed of a single green fluorescent protein. *Nature Biotechnology*, *19*(2), 137–41.

Nakamura, M., Baldwin, D., Hannaford, S., Palka, J., & Montell, C. (2002). Defective proboscis extension response (DPR), a member of the Ig superfamily required for the gustatory response to salt. *The Journal of Neuroscience : The Official Journal of the Society for Neuroscience*, *22*(9), 3463–3472.

Ni, L., Bronk, P., Chang, E. C., Lowel, A. M., Flam, J. O., Panzano, V. C., … Garitty, P. A. (2013). A gustatory receptor paralog controls rapid warmth avoidance in Drosophila. *Nature*, *500*(7464), 580–4.

Oka, Y., Butnaru, M., von Buchholtz, L., Ryba, N. J. P., & Zuker, C. S. (2013). High salt recruits aversive taste pathways. *Nature*, *494*(7438), 472–5.

Rajashekhar, K. P., & Singh, R. N. (1994b). Organization of motor neurons innervating the proboscis musculature in Drosophila melanogaster meign (diptera:Drosophilidae). *International Journal of Insect Morphology and Embryology*, *23*(3), 225–42.

Ramaekers, A., Parmentier, M.-L., Lasnier, C., Bockaert, J., & Grau, Y. (2001). Distribution of metabotropic glutamate receptor DmGlu-A inDrosophila melanogaster central nervous system. *The Journal of Comparative Neurology*, *438*(2), 213–25.

Reiter, S., Campillo Rodriguez, C., Sun, K., & Stopfer, M. (2015). Spatiotemporal Coding of Individual Chemicals by the Gustatory System. *Journal of Neuroscience*, *35*(35), 12309–21.

Robertson, H. M., Warr, C. G., & Carlson, J. R. (2003). Molecular evolution of the insect chemoreceptor gene superfamily in Drosophila melanogaster. *Proceedings of the National Academy of Sciences of the United States of America*, *100* (Suppl 2), 14537–42.

Scott, K., Brady, R., Cravchik, A., Morozov, P., Rzhetsky, A., Zuker, C., & Axel, R. (2001). A Chemosensory Gene Family Encoding Candidate Gustatory and Olfactory Receptors in Drosophila. *Cell*, *104*(5), 661–673.

Starostina, E., Liu, T., Vijayan, V., Zheng, Z., Siwicki, K. K., & Pikielny, C. W. (2012). A Drosophila DEG/ENaC subunit functions specifically in gustatory neurons required for male courtship behavior. *The Journal of Neuroscience*, *32*(13), 4665–74.

Stocker, R. F. (1994). The organization of the chemosensory system in Drosophila melanogaster: a rewiew. *Cell and Tissue Research*, *275*(1), 3–26.

Thistle, R., Cameron, P., Ghorayshi, A., Dennison, L., & Scott, K. (2012). Contact Chemoreceptors Mediate Male-Male Repulsion and Male-Female Attraction during Drosophila Courtship. *Cell*, *149*(5), 1140–1151.

Thorne, N., Chromey, C., Bray, S., & Amrein, H. (2014). Taste Perception and Coding in Drosophila. *Current Biology*, *128*(2), 189–190.

Toda, H., Zhao, X., & Dickson, B. J. (2012). The Drosophila Female Aphrodisiac Pheromone Activates ppk23+ Sensory Neurons to Elicit Male Courtship Behavior. *Cell Reports*, *1*(6), 599–607.

Venken, K. J. T., Simpson, J. H., & Bellen, H. J. (2011). Genetic manipulation of genes and cells in the nervous system of the fruit fly. *Neuron*, *72*(2), 202–230.

von Philipsborn, A. C., Liu, T., Yu, J. Y., Masser, C., Bidaye, S. S., & Dickson, B. J. (2011). Neuronal Control of Drosophila Courtship Song. *Neuron*, *69*(3), 509–522.

Vosshall, L. B., Amrein, H., Morozov, P. S., Rzhetsky, A., & Axel, R. (1999). A spatial map of olfactory receptor expression in the Drosophila antenna. *Cell*, *96*(5), 725–36.

Vosshall, L. B., & Stocker, R. F. (2007). Molecular architecture of smell and taste in Drosophila. *Annual Review of Neuroscience*, *30*, 505–533.

Walker, S. J., Corrales-Carvajal, V. M., & Ribeiro, C. (2015). Postmating Circuitry Modulates Salt Taste Processing to Increase Reproductive Output in Drosophila. *Current Biology*, *25*(20), 2621–2630.

Wang, Z., Singhvi, A., Kong, P., & Scott, K. (2004). Taste representations in the Drosophila brain. *Cell*, *117*(7), 981–991.

Weiss, L. A., Dahanukar, A., Kwon, J. Y., Banerjee, D., & Carlson, J. R. (2011). The molecular and cellular basis of bitter taste in Drosophila. *Neuron*, *69*(2), 258–272.

Wieczorek, H., & Wolff, G. (1989). The labellar sugar receptor of Drosophila. *Journal of Comparative Physiology A*, *164*(6), 825–834.

Xiang, Y., Yuan, Q., Vogt, N., Looger, L. L., Jan, L. Y., & Nung, Y. (2011). Light-avoidance-mediating photoreceptors tile the Drosophila larval body wall. *Nature*, *468*(7326), 921–926.

Yang, C. H., Belawat, P., Hafen, E., Jan, L. Y., & Jan, Y. N. (2008). Drosophila egg-laying site selection as a system to study simple decision-making processes. *Science*, *319*(5870), 1679–1683.

Zhang, Y. V, Ni, J., & Montell, C. (2013). The Molecular Basis for Attractive Salt Taste Coding in Drosophila Yali. *Science*, *340*(6138), 1334–1338.